Dicke Enhanced Energy Transfer via Off Resonant Coupling

by

Christopher Black

Submitted to the Department of Electrical Engineering and Computer Science
in Partial Fulfillment of the Requirements for the Degrees of
Bachelor of Science in Electrical Science and Engineering
and Master of Engineering in Electrical Engineering and Computer Science
at the Massachusetts Institute of Technology

November 19, 2000

Author _____
Department of Electrical Engineering and Computer Science
November 19, 2000

Certified by _____
Peter Hagelstein
Thesis Supervisor

Accepted by _____
Arthur C. Smith
Chairman, Department Committee on Graduate Theses

Dicke Enhanced Energy Transfer via Off Resonant Coupling
By
Christopher Black

Submitted to the
Department of Electrical Engineering and Computer Science

November 19, 2000

In Partial Fulfillment of the Requirements for the Degrees of
Bachelor of Science in Electrical Science and Engineering
and Master of Engineering in Electrical Engineering and Computer Science

ABSTRACT

This thesis examines the dynamics of energy exchange in a model for second-order (indirect) coupling through off-resonant states. Specifically, the model hosts a second-order transfer of energy between two collections of two level systems via an off-resonant oscillator. No first-order transfer of energy is possible because the systems are optically isolated. The entire system is placed into a low-frequency simple-harmonic-oscillator (SHO) which indirectly couples the two collections of systems. Therefore, if the SHO is removed there is no energy exchange.

The frequencies of the oscillator and two-level systems are different (off-resonant); therefore, the rates of exchange are expected to be quite low. This novel approach achieves measurable coupling through coherent enhancement analogous to Dicke's (1954) superradiance. This thesis examines the period and rate of energy-transfer between the isolated systems, and attempts to extract patterns that analytically depend upon the number of atoms in each cavity, the coupling strength, the photon level, and the off-resonant ratio parameter. The characterization that follows uses dimensionless quantities and therefore is applicable to many different applications of the model.

Thesis Supervisor: Peter Hagelstein
Title: Associate Professor, MIT Electrical Engineering, and Computer Science

TABLE OF CONTENTS

LIST OF FIGURES

Number *Page*

LIST OF TABLES

ACKNOWLEDGMENTS

The author wishes to thank Peter Hagelstein for the many ideas, insight, jar of peanut butter, futon, and intravenous caffeine setup. The author also wishes to thank John Fini for time above and beyond what was necessary, the numerous clear explanations, organizational input, and patience as I completed my thesis.

Most important of all, special thanks go to my lovely wife, Heather. She was patient with me while I spent all my time researching; she provided moral support, took care of the kids and the housework, proof-read, and of course made regular batches of cookies. This task would not have been possible without her overwhelming assistance! Last of all, I would like to thank my kids, Rebecca and Andrew, for sacrificing my extra time with them so that I could complete my thesis.

GLOSSARY

coherent: All atoms transition together in the same direction. A coherent excitation is when all atoms excite simultaneously.

coherent state: This expression is usually used in reference to a SHO. The wave packet follows classical motion similar to a pendulum and the shape of the wave packet remains constant. The generalized coherent state created in this thesis looks like a coherent state; however, it quickly loses its coherent properties (as would a coherent state in a quartic well).

gedanken experiment: gedanken is German for thought. A gedanken experiment refers to thinking through an experiment on paper.

off-resonance: If the energies/frequencies of coupled systems differ, their interaction is off-resonant.

sloshing: Energy dynamics that obscure the transfer of energy from system A to system B.

spinor: A two-element column matrix used to represent the general state of a spin-1/2 particle, or similarly (in pseudospin representation) used to represent the excitation state of a two-level system.

Chapter 1

INTRODUCTION

Scientists usually devise theory to explain existing physical systems that have not been described, or that need better, more accurate explanations.[1] This often provides us with tools to use the systems more effectively or more fully. However, sometimes it is useful to develop theory for systems that do not exist, in hopes that by understanding them we may bring them into existence. By understanding the underlying physics, researchers have been able to propose many new systems theoretically and then from the understanding gained by the theory, build them.

The system that we propose in this paper, as far as we know, does not exist. Hagelstein (1998) originally made the proposal in the late 1990s. The system investigates the use of coherent enhancement to strengthen a nominally weak process of off-resonant energy transfer. The model includes two off-resonant transfers, the first from a collection of two-level systems into an oscillator, and the second from the oscillator into a second collection of two-level systems. The two-level systems can represent a discrete transition for many different quantum systems; we use an atomic model, however the results are ubiquitous. Similarly, the oscillator can represent any system that rings with a lower frequency (necessary for coherent enhancement), such as a microwave field.

Hagelstein postulates that this system behaves similarly to coupled pendulums. If one pendulum is oscillating and the other at rest, after some time, the coupling

[1] The introduction is taken from (Hagelstein 1999), it has been paraphrased.

between the pendulums will transfer energy between them; therefore, the second pendulum will begin to oscillate. Eventually, the excitation from the first pendulum ideally is transferred to the second pendulum. The transfer of energy repeats itself and oscillates back and forth. Each pendulum may be ringing; however, independent of its motion, the overall energy oscillates between them.

The pendulum illustration gives an easily understood and insightful representation of the system. We now proceed with a gedanken experiment (see Figure 1) to provide insight into the physical implementation of the model.

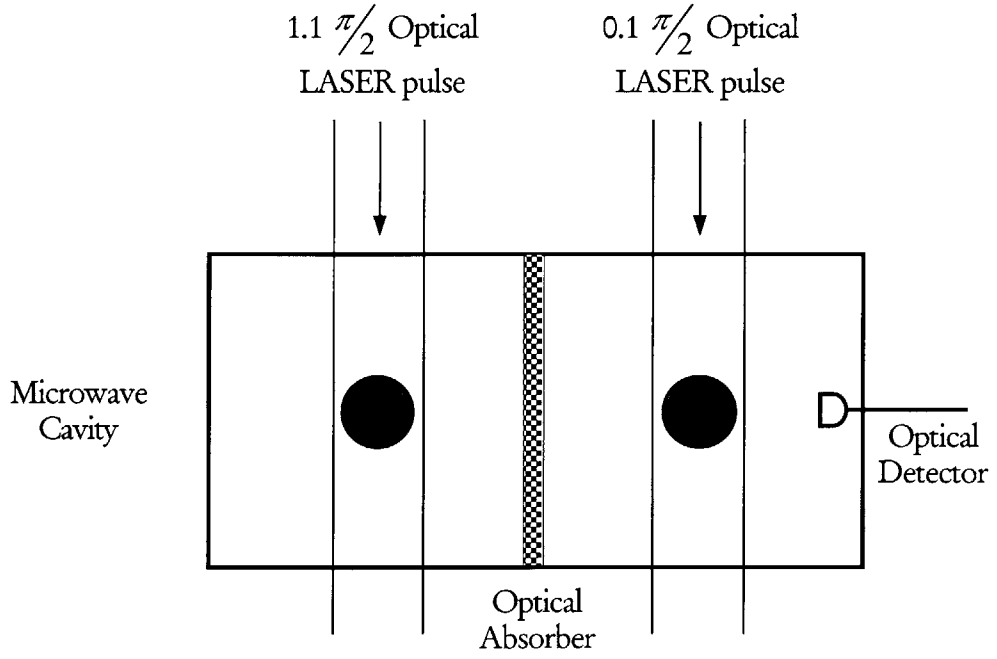

Figure 1: Schematic of a gedanken experiment

Figure from (Hagelstein 1999), used with permission.

This experiment uses atomic transition for the two-level systems and a microwave cavity for the oscillator. In a real system, the atoms would radiatively decay with a lifetime depending upon both the material and the discrete transition. We assume in our model that the coherent dynamics are much quicker than this lifetime. When implementing our system, this concern will affect the choice of materials for the gas.

Ignoring the decay mechanisms, our model predicts that excitation transfers between the two systems. However, this is not obvious from our setup, because the two cavities are optically isolated. The optical absorber is transparent to the microwave field, and so the exchange of energy occurs via the microwave field. The mechanism of exchange is off-resonant photons. One system emits an off-resonant photon, and the other system absorbs it. This channel of exchange is expected to be quite weak, so the expectation that these off-resonant processes should be significant goes against intuition, and demands more explanation.

The weak indirect coupling between the collections of two-level systems may not be expected to satisfy our earlier assumption that the dynamics of exchange were quicker than the radiative-decay lifetime of the atoms. However, this is where our model differs from previous examinations of this type of effect. Since the wavelength of the oscillator is much longer than the optical cavity, we can generate substantial coherence factors. Therefore, the effective interaction strength is much larger than expected—directly analogous to Dicke superradiance (for more information see Dicke's paper (1954)).

The proposal of off-resonant supperradiant effects suggests a model for a system that does not yet exist. This theoretical exercise examines the plausibility of one such physical model. We believe that the theory demonstrates that the system is not only possible but also measurable, and that we may facilitate its existence with appropriate experiments. If the theory proves to be correct, this new physical

model would have many possible applications. We could create a laser that would exploit this ability to transfer by coupling a large system that is relatively unexcited into smaller systems. In addition, Hagelstein further suggest applications in spectroscopy, and up-conversion and down-conversion during nonlinear excitation transfer. (Hagelstein 1999)

Chapter 2

MODEL

The model consists of three components: two cavities of gaseous atoms or molecules (two-level systems) that are isolated from each other, and an electromagnetic field (SHO) which is off-resonant. Figure 2 illustrates the system with two pictures: a structural diagram and functional diagram. The two cavities are identical; they each have the same number of atoms and equivalent coupling parameters. Initially, a laser excites Cavity *A* at the transition frequency. The atoms in the cavity are modeled as a collection of two-level systems; therefore, the excitation energy is chosen respective to the energy of the gas in the cavity. The electromagnetic field is any off-resonant field, such as a microwave, that can be modeled as an oscillator.

Hamiltonian

The total Hamiltonian models the collections of two-level systems, the oscillator, and the coupling between the components. The collections of two-level systems (*A* and *B*) are isolated from each other; therefore, the coupling term between them is zero. However, they each couple with the oscillator. Equation (2.1) shows an appropriate Hamiltonian for the system.

$$\hat{H} = \overbrace{\frac{\Delta E}{2}\hat{\Sigma}_z^A}^{\text{Two-Level Systems 'A'}} + \overbrace{\frac{\Delta E}{2}\hat{\Sigma}_z^B}^{\text{Two-Level Systems 'B'}} + \overbrace{\hbar\omega_0\hat{a}^\dagger\hat{a}}^{\text{Oscillator Field}} + \underbrace{V_A\left(\hat{a}+\hat{a}^\dagger\right)^k\hat{\Sigma}_x^A}_{\text{Coupling of 'A' and Oscillator}} + \underbrace{V_B\left(\hat{a}+\hat{a}^\dagger\right)^k\hat{\Sigma}_x^B}_{\text{Coupling of 'B' and Oscillator}} \tag{2.1}$$

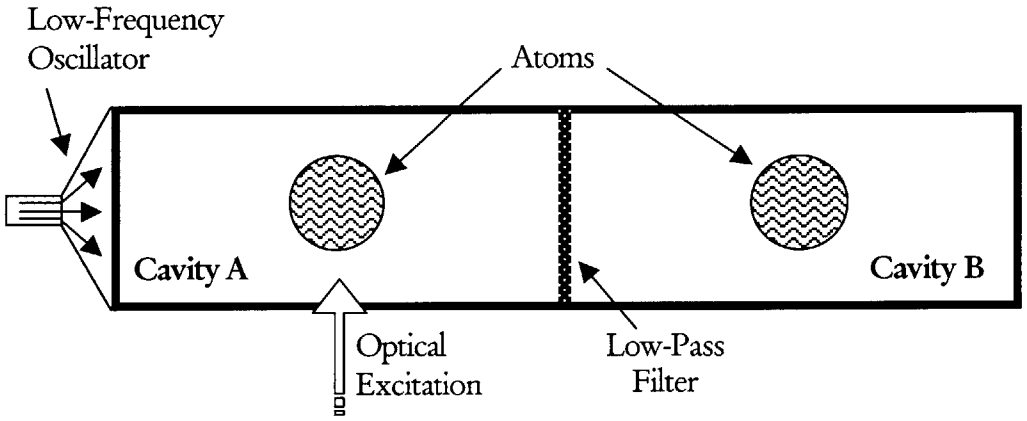

(a)

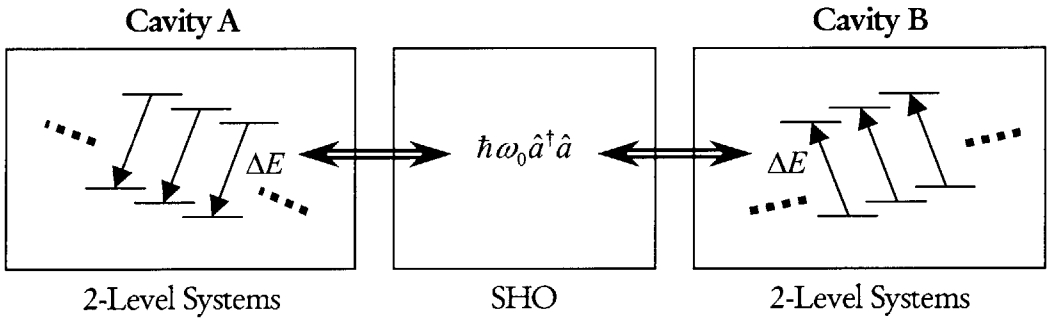

(b)

Figure 2: (a) Top-level Diagram of Model (b) Functional Diagram of Model

We use standard creation and annihilation operators to describe photon exchange in the oscillator. The resonant energy of the oscillator is $\hbar\omega_0$; its zero-state energy is unimportant, and consequently not modeled. The transition energy for the two-level systems is ΔE, and the model assumes that transitions in any atom are produced with equal probability. V_A and V_B represent the coupling strengths, and are equal for the described setup. The oscillator component of the coupling parameter is to the k power, which allows for higher order photon exchange. If a simple electromagnetic wave such as a microwave is used for the oscillator, k is equal to one; however, in other applications, for example atoms or molecules coupled to a phonon field, a higher order k of twenty or thirty may be necessary.

Pseudospin Atomic Model

The basic atomic model uses the same pseudospin formalism for the two-level systems as in Hagelstein's (1998) earlier paper. A two-element column vector (or **spinor**) models the two-level system. Each element represents one of the two states of the atom. If the value is one, then the atom is in that state; otherwise, it is equal to zero.

$$\begin{aligned} \text{Unexcited:} \quad & \begin{bmatrix} 0 \\ 1 \end{bmatrix} \\ \text{Excited:} \quad & \begin{bmatrix} 1 \\ 0 \end{bmatrix} \end{aligned} \tag{2.2}$$

The state vectors for the atoms multiply together to form a product state for the system.

$$\prod_i \begin{bmatrix} x \\ y \end{bmatrix}_i \tag{2.3}$$

For a single two-level atom, an arbitrary operator can be composed of the Pauli spin matrices $\hat{\sigma}_x$, $\hat{\sigma}_y$, and $\hat{\sigma}_z$. $\hat{\sigma}_z$ leaves the atomic excited or unexcited state invariant, and $\hat{\sigma}_x$ produces an atomic transition between the two states.

$$\hat{\sigma}_z = \begin{bmatrix} 1 & 0 \\ 0 & -1 \end{bmatrix} \tag{2.4}$$

$$\hat{\sigma}_x = \begin{bmatrix} 0 & 1 \\ 1 & 0 \end{bmatrix} \tag{2.5}$$

Note: $$\hat{\sigma}_x = \hat{\sigma}_+ + \hat{\sigma}_- = \begin{bmatrix} 0 & 1 \\ 0 & 0 \end{bmatrix} + \begin{bmatrix} 0 & 0 \\ 1 & 0 \end{bmatrix} \tag{2.6}$$

To describe coherent excitation of many atoms, we use the following pseudospin operators:

$$\hat{\Sigma}_z = \sum_i \hat{\sigma}_z(i) = \sum_i \begin{bmatrix} 1 & 0 \\ 0 & -1 \end{bmatrix}_i \tag{2.7}$$

$$\hat{\Sigma}_x = \sum_i \hat{\sigma}_x(i) = \sum_i \begin{bmatrix} 0 & 1 \\ 1 & 0 \end{bmatrix}_i \tag{2.8}$$

Representation of System States

The two-element column matrix (or spinor) notation of equations (2.2) and (2.3) is not convenient when greater than a few atoms are used; therefore, we will use a simple notation to represent the system states. The eigenstates of the system depend not only on the number of atoms that are excited in each cavity, but also on the number of photons in the SHO; they in general look like

$$\Phi = \sum_{n}\sum_{M_a}\sum_{M_b} C_{nM_aM_b} \left|S_a M_a\right\rangle \left|S_b M_b\right\rangle \phi_n \tag{2.9}$$

Three parameters are necessary to specify an eigenstate of the system: the photon level, *n*; the number of excited atoms in cavity *A*, M_1; and the number of excited atoms in cavity *B*, M_2. The photon number *n* is straightforward. The remaining parameters, S and M, function like spin eigenstates; they are calculated using Dicke algebra. This formulation is useful for this project because "the energy trapping which results from the internal scattering of photons by the gas appears naturally in the formalism." (Dicke, 1954, p. 102) In spin notation, every elementary particle has a specific fixed value of S, which represents the *spin* of that particular species. (Griffeths, 1995, p. 154) Similarly, the Dicke S is fixed; it may include half-integral values and it represents the total number of atoms in a particular cavity. M is equivalent to the spin eigenstate; it ranges from positive to negative S, and can only change by the integer one when a transition operator is applied to it.

$$\Delta M = \pm 1 \tag{2.10}$$

However, note that M is integral only if the number of atoms is even. From this formulation, physical definitions for S and M follow:

$$S = \frac{1}{2}\text{Atoms} \tag{2.11}$$

$$M = \frac{1}{2}\left(\text{Atoms}_{\text{Excited}} - \text{Atoms}_{\text{Unexcited}}\right) \tag{2.12}$$

(Note: The definition for S includes only the number of atoms in phase; if the atoms are out of phase, they cancel giving a lower effective S.)

Dicke Algebra

1-Atom Coefficients

The operators described above generate coefficients when applied to an eigenstate. Let us use an unexcited one-atom example to determine the coefficients created by these new operators. From equations (2.4) to (2.8), the one-atom operators are

$$\hat{\Sigma}_z = \hat{\sigma}_z = \begin{bmatrix} 1 & 0 \\ 0 & -1 \end{bmatrix} \tag{2.13}$$

$$\hat{\Sigma}_+ = \hat{\sigma}_+ = \begin{bmatrix} 0 & 1 \\ 0 & 0 \end{bmatrix} \tag{2.14}$$

$$\hat{\Sigma}_- = \hat{\sigma}_- = \begin{bmatrix} 0 & 0 \\ 1 & 0 \end{bmatrix} \tag{2.15}$$

From equations (2.11) and (2.12) the initial eigenstate for an unexcited single-atom system is

$$\phi_i = |S, M_i\rangle = \left|\frac{1}{2}, -\frac{1}{2}\right\rangle \tag{2.16}$$

Let us first apply the normalized energy operator, (2.13), to the eigenstate, (2.16), to determine its coefficient.

$$\hat{\Sigma}_z \left|\frac{1}{2}, -\frac{1}{2}\right\rangle = \begin{pmatrix} 1 & 0 \\ 0 & -1 \end{pmatrix}\begin{pmatrix} 0 \\ 1 \end{pmatrix} = \begin{pmatrix} 0 \\ -1 \end{pmatrix} = (-1)\left|\frac{1}{2}, -\frac{1}{2}\right\rangle \tag{2.17}$$

(Note: in equation (2.17), the vector notation and the eigenstate notation is used interchangeably.) The coefficient from equation (2.17) is equal to $2M$.

$$\hat{\Sigma}_z |S,M\rangle = 2M |S,M\rangle \tag{2.18}$$

This relation holds for all values of S and M.

The Σ_x operator changes the state of the atom; therefore, since the atom is initially unexcited, applying the increment operator (2.14) yields an excited atom.

$$\hat{\Sigma}_+ \left|\frac{1}{2},-\frac{1}{2}\right\rangle = \begin{pmatrix} 0 & 1 \\ 0 & 0 \end{pmatrix}\begin{pmatrix} 0 \\ 1 \end{pmatrix} = \begin{pmatrix} 1 \\ 0 \end{pmatrix} = \left|\frac{1}{2},\frac{1}{2}\right\rangle \tag{2.19}$$

From equation (2.19), the coefficient for this single atom example is one. However, the coefficient changes depending upon the current state and the number of atoms; therefore, more examples are necessary to determine the analytic value of the coefficient.

Multi-Atom Coefficients

For the two-atom case

$$\hat{\Sigma}_z = \begin{pmatrix} 1 & 0 \\ 0 & -1 \end{pmatrix}_1 + \begin{pmatrix} 1 & 0 \\ 0 & -1 \end{pmatrix}_2 \tag{2.20}$$

$$\hat{\Sigma}_+ = \begin{pmatrix} 0 & 1 \\ 0 & 0 \end{pmatrix}_1 + \begin{pmatrix} 0 & 1 \\ 0 & 0 \end{pmatrix}_2 \tag{2.21}$$

$$\hat{\Sigma}_- = \begin{pmatrix} 0 & 0 \\ 1 & 0 \end{pmatrix}_1 + \begin{pmatrix} 0 & 0 \\ 1 & 0 \end{pmatrix}_2 \tag{2.22}$$

Using equations (2.11) and (2.12), the initial eigenstate when both atoms are initially unexcited is

$$\phi_i = |S, M_i\rangle = |1, -1\rangle \tag{2.23}$$

Applying operator (2.21) to the initial state (2.23) yieldsone excited atom and one unexcited atom.

$$\hat{\Sigma}_+ |1,-1\rangle = \left(\begin{bmatrix} 0 & 1 \\ 0 & 0 \end{bmatrix}_1 + \begin{bmatrix} 0 & 1 \\ 0 & 0 \end{bmatrix}_2 \right) \begin{bmatrix} 0 \\ 1 \end{bmatrix}_1 \begin{bmatrix} 0 \\ 1 \end{bmatrix}_2 = \begin{bmatrix} 1 \\ 0 \end{bmatrix}_1 \begin{bmatrix} 0 \\ 1 \end{bmatrix}_2 + \begin{bmatrix} 0 \\ 1 \end{bmatrix}_1 \begin{bmatrix} 1 \\ 0 \end{bmatrix}_2 \tag{2.24}$$

The final state has one excited and one unexcited atom, so $|1,0\rangle$ is the expected final state. Since, either atom can be excited with equal probability, $|1,0\rangle$ must combine and normalize both possible outcomes.

$$|1,0\rangle = \frac{1}{\sqrt{2}} \begin{bmatrix} 1 \\ 0 \end{bmatrix}_1 \begin{bmatrix} 0 \\ 1 \end{bmatrix}_2 + \frac{1}{\sqrt{2}} \begin{bmatrix} 0 \\ 1 \end{bmatrix}_1 \begin{bmatrix} 1 \\ 0 \end{bmatrix}_2 \tag{2.25}$$

Comparing equations (2.24) and (2.25), the coefficient must be $\sqrt{2}$

$$\hat{\Sigma}_+ |1,-1\rangle = \begin{bmatrix} 1 \\ 0 \end{bmatrix}_1 \begin{bmatrix} 0 \\ 1 \end{bmatrix}_2 + \begin{bmatrix} 0 \\ 1 \end{bmatrix}_1 \begin{bmatrix} 1 \\ 0 \end{bmatrix}_2 = \sqrt{2} |1,0\rangle \tag{2.26}$$

Table 1 includes all coefficients for up to three atoms. The general relation is:

$$\Sigma_\pm |S, M\rangle = \sqrt{S(S+1) - M(M \pm 1)} |S, M \pm 1\rangle \tag{2.27}$$

Table 1: Dicke Coefficients for Differing Number of Atoms

	S	M	Operator	Coefficient
1-Atom	$\frac{1}{2}$	$-\frac{1}{2}$	Σ_-	0
	$\frac{1}{2}$	$-\frac{1}{2}$	Σ_+	1
	$\frac{1}{2}$	$\frac{1}{2}$	Σ_-	1
	$\frac{1}{2}$	$\frac{1}{2}$	Σ_+	0
2-Atom	1	-1	Σ_-	0
	1	-1	Σ_+	$\sqrt{2}$
	1	0	Σ_-	$\sqrt{2}$
	1	0	Σ_+	$\sqrt{2}$
	1	1	Σ_-	$\sqrt{2}$
	1	1	Σ_+	0
3-Atom	$\frac{3}{2}$	$-\frac{3}{2}$	Σ_-	0
	$\frac{3}{2}$	$-\frac{3}{2}$	Σ_+	$\sqrt{3}$
	$\frac{3}{2}$	$-\frac{1}{2}$	Σ_-	$\sqrt{3}$
	$\frac{3}{2}$	$-\frac{1}{2}$	Σ_+	2
	$\frac{3}{2}$	$\frac{1}{2}$	Σ_-	2
	$\frac{3}{2}$	$\frac{1}{2}$	Σ_+	$\sqrt{3}$
	$\frac{3}{2}$	$\frac{3}{2}$	Σ_-	$\sqrt{3}$
	$\frac{3}{2}$	$\frac{3}{2}$	Σ_+	0

Chapter 3

DYNAMICS

Chapter 2 gives us a framework for discussing energy in the three subsystems—M_1, M_2, and n. This chapter examines the evolution of the energy in the subsystems over time. The expectation of $\hat{\Sigma}_z^A$ and $\hat{\Sigma}_z^B$ represents the instantaneous localized energies in the cavities. Therefore, by scaling, we can monitor the energy of the cavities through the excitation number, M. We define two new expectations.

$$\left\langle \hat{M}_1 \right\rangle \equiv \frac{1}{2}\left\langle \hat{\Sigma}_z^A \right\rangle$$
$$\left\langle \hat{M}_2 \right\rangle \equiv \frac{1}{2}\left\langle \hat{\Sigma}_z^B \right\rangle \tag{3.1}$$

In the absence of coupling, the system evolves trivially, $\langle M_1 \rangle$ and $\langle M_2 \rangle$ remain constant. However, with coupling, we expect to see periodic transfer of energy between cavity A and cavity B. Figure 3 schematically illustrates the path we expect the energy to take. We are interested in the system with coupling, and specifically the details of the transition of energy from cavity A to cavity B. How sinusoidal is the transfer between the cavities? At what rate does it transfer? What system parameters define the period of motion?

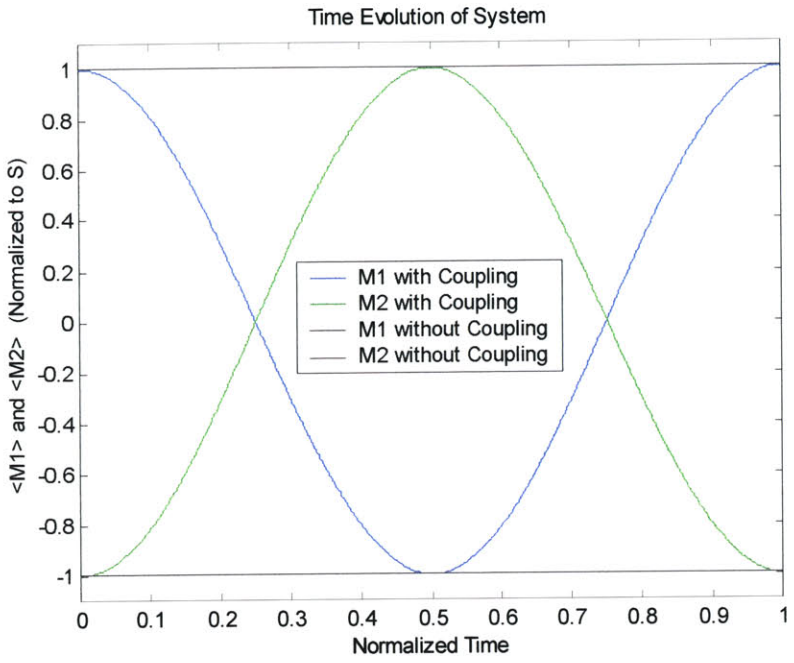

Figure 3: Expected Energy Evolution With and Without Coupling

Evolution of States

Outlining the periodic energy activity between the initial and final state requires examining the time evolution of the energy in the system. Beginning with a relevant basis of states

$$\left|\phi_j\right\rangle \tag{3.2}$$

the resulting finite basis approximation for the Hamiltonian is found from

$$H_{ij} = \left\langle \phi_i \middle| \hat{H} \middle| \phi_j \right\rangle \tag{3.3}$$

The energies of the system are the corresponding eigenvalues of the finite basis matrix. Each eigenvector describes the energy contributions from each state. Therefore, solving the Hamiltonian (3.3) for eigenvalues and eigenvectors give

$$\underbrace{H}_{\text{Matrix}} \overbrace{v_k}^{\text{Vector}} = \underbrace{E_k}_{\text{Scalar}} v_k \tag{3.4}$$

Let u be the probability amplitude of the system. u has a time-dependent component for each state of the basis, that component is the instantaneous probability amplitude of its respective state. For example, if the system is initialized in the third basis state, (ϕ_3), then $u(t=0)$ is

$$u(t=0) = \begin{bmatrix} 0 \\ 0 \\ 1 \\ 0 \\ \vdots \\ 0 \end{bmatrix} \tag{3.5}$$

We would like to make use of the following identity matrix:[1]

$$I = \sum_k |k\rangle\langle k| = \sum_k v_k v_k^\dagger \tag{3.6}$$

---

[1] Note the symbol, †, in this context is not the 'dagger' operator but the adjoint operator. The adjoint of a vector/matrix is the complex conjugate transpose.

$$\left.\begin{array}{l} |A\rangle^\dagger = \langle A| \\ \begin{bmatrix} a_1 \\ \vdots \\ a_n \end{bmatrix}^\dagger = \begin{bmatrix} a_1^* \cdots a_n^* \end{bmatrix} \end{array}\right\} \langle A|A^\dagger\rangle = |a_1|^2 + \cdots + |a_n|^2 \underbrace{=}_{\substack{\text{For} \\ \text{Normalized} \\ \text{Eigenvectors}}} 1$$

Multiplying equation (3.5) by equation (3.6) gives:

$$u(0)=\left(\sum_k v_k v_k^\dagger\right)u(0) \tag{3.7}$$

In vector form, equation (3.7) is a column multiplied by a row that is multiplied by a column. The last two components, the row times a column, is a dot product and simplify to a constant; therefore, it can be moved before the first column.

$$u(0)=\sum_k\left[\left(v_k^\dagger u(0)\right)v_k\right] \tag{3.8}$$

The evolution of this state vector is given by:

$$u(t)=e^{-i\frac{\hat{H}}{\hbar}t}\cdot u(0)=e^{-i\frac{\hat{H}}{\hbar}t}\sum_k\left[\left(v_k^\dagger u(0)\right)v_k\right]=\sum_k\left[\left(v_k^\dagger u(0)\right)e^{-i\frac{E_k}{\hbar}t}v_k\right] \tag{3.9}$$

Energy Initialization

The choice of $u(0)$ in equation (3.9) significantly affects the dynamics of energy transfer. If the energy is initialized into states that do not couple with the set of states that we are interested in, then the evolution is trivial; because no energy ever evolves into the relevant states. Therefore, the initial state must be chosen carefully so that the energy is optimized to transfer back and forth from cavity *A* to cavity *B*.

Single-State Initialization of Energy Eigenvalues

One approach to initialization is to place all of the energy into a single basis state $|\phi\rangle$. If we initialize all of the energy in cavity *A*, such that all its atoms are

excited, $|S,S\rangle_A|S,-S\rangle_B$, then we could expect that the energy would transfer to cavity ***B***. Therefore, keeping the photon level at its center, this approach gives the following initial state:

$$|S,S\rangle_A|n_0\rangle|S,-S\rangle_B \tag{3.10}$$

Let this be the l^{th} state of our basis, ϕ_l, then the initial state, $u(0)$, is all zeros with a one in the l^{th} location. From equation (3.9), the probability amplitude for the m^{th} state, given that the energy is initially placed in the l^{th} state, is

$$u_m = \sum_k \left[\underbrace{v^*_{k,l}}_{\substack{k\,\text{vector} \\ l\,\text{entry}}} \cdot e^{-i\frac{E_k}{\hbar}t} v_{k,m} \right] \tag{3.11}$$

Gaussian Initialization of Energy Eigenvalues

The initialization chosen in equation (3.11) is good because it guarantees that one of the states that we are interested in has energy; however, it is poor because it introduces extra sloshing to the system. Let us take a moment to clarify what we mean by 'extra sloshing'. When the system has many rapid dynamics that do not cause excitation from system *A* to system ***B***, the transfer of energy appears somewhat chaotic. This chaotic energy transfer sloshes around; hence 'extra sloshing'.

We would like to eliminate the sloshing from the system. Initializing all the energy of the system into a single state is far from the system's equilibrium point; therefore, the system has extraneous rapid dynamics. If we initialize the system with the energy balanced similar to equilibrium; then we will significantly reduce

the extra sloshing. We attempt to simulate this effect with a Gaussian weighting of the eigen-energies for the system.

Implementation of Gaussian Filter

Let us begin by examining the effect of coupling using the eigenstates of the uncoupled system as a basis.

$$H_0\phi_j = \varepsilon_j\phi_j \tag{3.12}$$

We can also write the coupled eigenstates.

$$(H_0 + V)v_j = E_j v_j \tag{3.13}$$

The proposal is to let

$$u'(t=0) = \sum_j c_j v_j \tag{3.14}$$

where c_j simulate the equilibrium conditions of the system. However, the system is rather complex, and we do not know the equilibrium spread of energy. Therefore, we can make an educated guess that it is close to a Gaussian, and let

$$c_j = e^{-\alpha(E_j - E_{\text{Central}})^2} \tag{3.15}$$

We expect a Gaussian to simulate the equilibrium point closely enough to see the periods clearly; however, a Gaussian is not sufficient by itself. We need an initial state that localizes energy in system A. Therefore, we combine the Gaussian weighting with the original basis state $|\phi_j\rangle$.

$$u(t) = \sum_k \frac{\left[v_k^\dagger \tilde{u}_0\right] e^{-\alpha(E_k - E_{Center})^2} e^{-i\frac{E_k}{\hbar}t} \vec{v}_k}{\mathrm{N}} \tag{3.16}$$

where the normalization constant N is

$$\mathrm{N} = \sqrt{\sum_k \left[v_k^\dagger \tilde{u}_0\right]^2 e^{-2\alpha(E_k - E_{\mathrm{Center}})^2}} \tag{3.17}$$

and

$$E_{\mathrm{Center}} = \frac{\sum_i^{\mathrm{B}} E_i}{\mathrm{B}} = Mean(E) \tag{3.18}$$

We want to favor cavity A so that the largest amplitude of oscillation is between cavity A and B. Therefore, we let the initial favored state be $\phi_l = |S,S\rangle_A |n\rangle |S,-S\rangle_B$.

$$\tilde{u}_0 = \begin{bmatrix} 0 \\ \vdots \\ 0 \\ 1 \\ 0 \\ \vdots \\ 0 \end{bmatrix} \leftarrow \phi_l \tag{3.19}$$

For a correct choice of the Gaussian parameter, α, this formulation successfully distributes the initial energy across the eigenvalues such that sloshing is minimal and the energy is mostly initialized in the proposed initial state, $\tilde{u}_0$.

"In essence, choosing coefficients to resolve $\phi_I = |S,S\rangle_A |n\rangle |S,-S\rangle_B$ leads to rapid dynamics that do not cause transfer of excitation from system *A* to system *B*. We add a Gaussian filter to suppress this effect." (Hagelstein, personal communication, October 27, 2000)

See Appendix A for this model in a Matlab *m*-file.

Chapter 4

NUMERICAL IMPLEMENTATION

Complete Basis Set

Our next task is to choose a basis with which to work. The system has three degrees of freedom: M_A, M_B, and n. The size of the M-axes depends only upon the number of atoms in the system. M_A and M_B are identical in construction. Each atom is either excited or unexcited (two states per atom); therefore, one would expect that the total number of states for each M-axis is 2^A. However, all atoms in the system interact with the oscillator in the same way, so they are indistinguishable from each other—either 0 atoms are excited, or 1, or 2,..., or A atoms. This is a total of $A+1$ states. We can also calculate this value numerically from Dicke algebra. We know that M can change by the integer one, and ranges from $-S$ to S:

$$M \in \{-S, -S+1, ..., S-1, S\} \tag{4.1}$$

Therefore, there are $2S+1$ possible states for each M-axis. Since $S = \frac{A}{2}$,

$$\#States_{M_x} \equiv \#_{M_x} = A+1 \tag{4.2}$$

There are two dimensions for M, so the total cross-sectional state area for the M-plane is

$$\#States_M = \#_{M_a} \cdot \#_{M_b} = (A+1)^2 \tag{4.3}$$

The size of the n-axis is infinite; there can be anywhere from zero to an infinite number of photons in the resonator.

Therefore, our complete basis set is a four-sided column of cross-sectional area $(A+1)^2$ that begins at $n=0$ and continues to infinity. Clearly, an infinite basis set is not practical for this problem, nor computationally feasible. However, we can reduce the size of the basis once we examine the coupling pathways more closely.

Finite Basis Set

There are two states of particular interest in our problem. Initially, we are interested in all the atoms in cavity A being excited and cavity B unexcited. The other state of interest is the complement to the first state: all atoms in cavity A unexcited, and cavity B excited.

State I Cavity A: excited, $|S,S\rangle_A$; Cavity B: unexcited, $|S,-S\rangle_B$

State II Cavity A: unexcited, $|S,-S\rangle_A$; Cavity B: excited, $|S,S\rangle_B$

We are interested in these two states, because they are the endpoints of a complete energy transfer from cavity A to Cavity B. Let us begin with these two states as our finite basis, and then include those states that couple with them.

Determining the states that couple, require us reexamine the Hamiltonian, equation (2.1). The first three components do not cause transitions (between basis states), and therefore can be ignored for this discussion; however, the last two terms do. The pseudo-spin operators change either the excitation parameter

in cavity A, M_A, or in cavity B, M_B, by one. Similarly, the creation and annihilation operators change the photon level, n; however, with the k-order parameter, the exchange is not as simple. The photon exchange can be any other number from $-k$ to $+k$. For example, if $k=1$, then $n_{new}=n\pm1$; however, if $k=2$, then $n_{new}=0$ or ±2. See Table 2.

Let us examine the one-atom case, $A=1$, with $k=1$. To facilitate the graphic representation, we combine M_A and M_B into a single axis M. This is possible, since each axis is finite, and gives us a new axis of length $(A+1)^2=4$. Using a slightly modified M-notation of $|M_A,M_B\rangle$, State I and State II are now $\left|\frac{1}{2},-\frac{1}{2}\right\rangle|n\rangle$ and $\left|-\frac{1}{2},\frac{1}{2}\right\rangle|n\rangle$, respectively. From Table 2, we can say that State I couples with four other states: $\left|-\frac{1}{2},-\frac{1}{2}\right\rangle|n\pm1\rangle$ and $\left|\frac{1}{2},\frac{1}{2}\right\rangle|n\pm1\rangle$. Figure 4 maps out all states that couple with State I and State II for five photon levels. The coupling continues down to $n=0$ and up to $n\to\infty$. The blue lines in Figure 4 represent the coupling pathways defined by the interaction Hamiltonian (3.3). All other states may be excluded.

Table 2: Possible Coupling Pathways

	Axis	Change
	M_A	±1
	M_B	±1
	n	$-k,-k+2,\cdots,k-2$, or k
Logic	$(\Delta M_A$ OR $\Delta M_B)$ AND Δn	

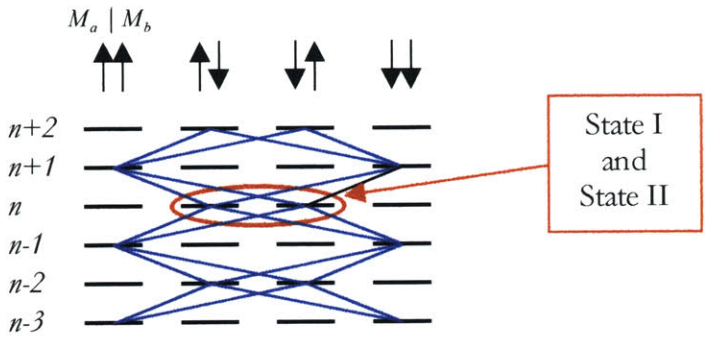

Figure 4: Coupling Map of Possible States

We have cut in half the number of states in the basis; however, it is still infinite. On the *n*-axis, the closer states couple stronger than the distant states, so if the contributions of these states become small enough, we can ignore them. However, what defines the coupling of a state to be small enough? This question depends upon the coupling strength, the photon level, and the off-resonant energy ratio. We determine it computationally by adding photon levels until the results do not change.

The convention this paper uses numbers the basis set from left to right and top to bottom, where only the states that couple (touched by a blue line) are included. If the example that is in Figure 4 were used the basis would have 12 states; these are numbered in Figure 5.

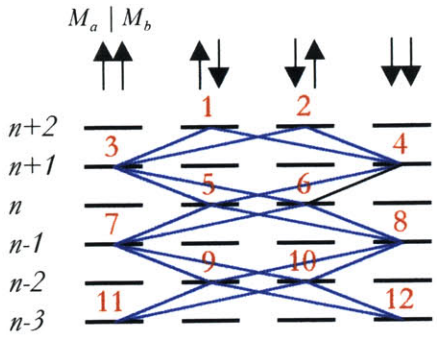

Figure 5: Basis Numbering Convention

In Appendix B, matlab code is attached that creates a basis and calculates the respective Hamiltonian.

Photon Level Span in Basis

Each photon level added increases the total number of states by four. To simplify the following discussion, we define a new variable l.

$$l = n - n_0 \tag{4.4}$$

Where n_0 is the photon level of the system initially, and n is the photon level of the current state. We generate the basis symmetrically around the initial photon level, n_0; therefore, for a given l, the span in n is $2l+1$. To monitor the probability of occupation in each photon level, we sum the occupational probabilities of each state within a photon level and average over all time. Then we graph on a log-linear plot the sum versus relative photon level, l. Such a graph tells us how many photon levels participate significantly, and how many must be included for accurate modeling.

There are typically two parts to every curve. The first segment does an initial drop and then wiggles around an occupation level up unto some l. The second segment falls off exponentially. If we include enough states, at some l the curve eventually levels off due to truncation error within the computer; this is an artifact of the computer, not the quantum system. In the first segment, the occupation level is jumping around, and therefore, can still change the dynamics considerably (depending on the magnitude of the occupation). However, when the second segment of the curve begins its path becomes predictable, and we can anticipate any changes in dynamics. In other words, there will be no sudden period fluctuations when the basis is expanded past this point. The point, l, where the second segment of the curve begins (where its path becomes predictable) is the theoretical point we choose to accurately describe the dynamics of the system.

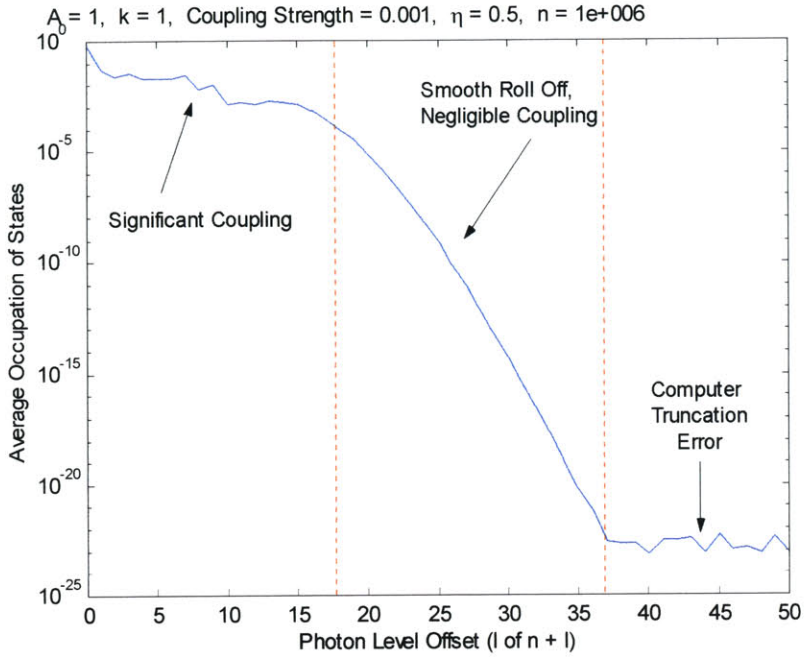

Figure 6: System I—Average Occupation per Photon Level

See Figure 6 for a one-atom example of the photon curve. This curve uses single-state initialization with its initial parameters labeled above the graph. Notice the two segments of the curve that we have described. Based upon this graph, we would generally choose an l in the range of 20 to 30 for this system; this choice is safely above the error threshold. The truncation error jumps around, but its average value stays very constant. In addition, its occupation value will generally be below 10^{-25}.

Unfortunately, the photon curve is not always as clear as the above graph, so choosing the breakpoint is not always possible or sufficient for accurate results. Figure 7, Figure 8, and Figure 9 show a few of these variations. The figures all have significant ripple on the smooth roll off section. Our argument is that we have included all significant coupling because the curve becomes predictable and small; this is no longer true, for the occupation level bounces around what we

expect. Figure 8 adds another difficulty, for it does not reach the roll off section until l equals 260. This high value is computationally prohibitive for any atomic value other than one. Figure 9 also requires an enormous basis to reach the roll off point; furthermore, the jitter is large and does not attenuate.

First, we must quantify the error associated with the ripple. If the error is low enough, then it may allow us to reduce the number of photon levels that we generally include for a system. Let us first characterize how the period changes as we expand the number of photon levels included in the basis. Table 3 includes the four systems shown in Figure 6, Figure 7, Figure 8 and Figure 9 over important values of l. Table 3 shows that it is quite possible to achieve good answers with even less photon levels than earlier proposed for many of the systems. However, System IV varies widely over the change in photon level; therefore, special care must be taken when the large characteristic zigzag of this system is seen. In the large coupling limit $\left(\text{when } g\sqrt{n} > 1\right)$, these zigzags become more common, and significantly interfere with data collection. Unfortunately for the other systems, the measurement error of the periods is close to that shown between photon levels for each system. Therefore, we are less sensitive to the finite basis error and cannot achieve very precise mappings of the periods. However, our level of accuracy is more than sufficient to analytically define the system.

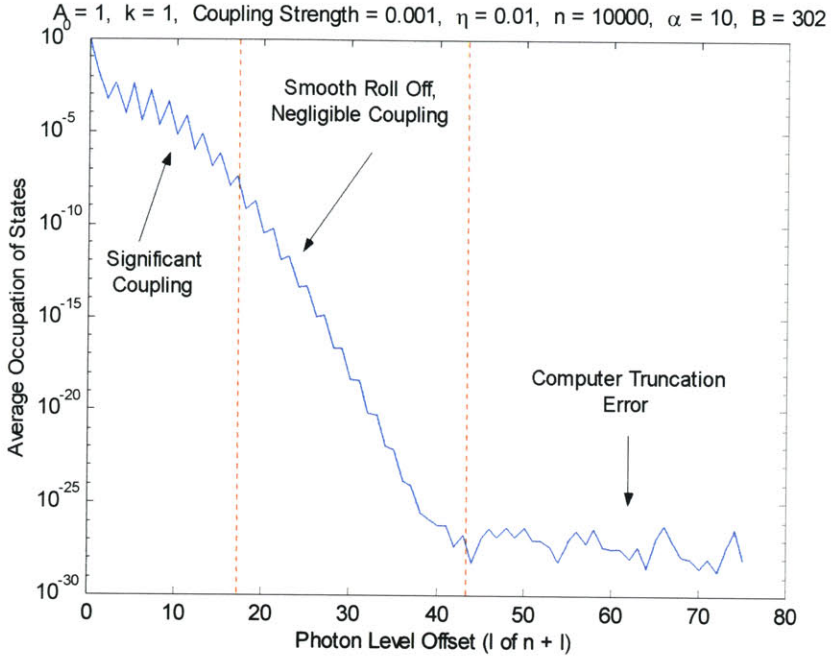

Figure 7: System II—Ripple on the Second Segment, Instead of a Smooth Drop Off.

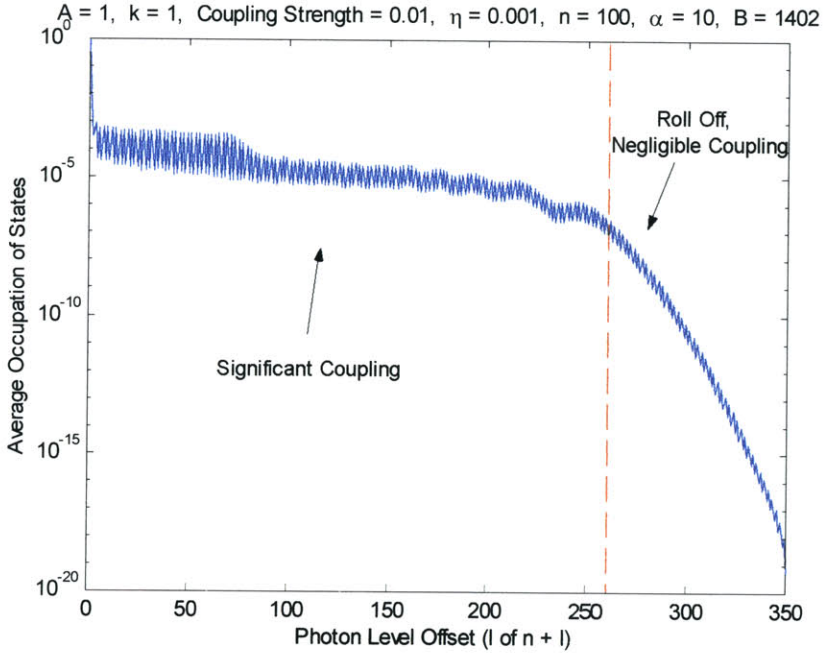

Figure 8: System III—The Curve Never Reaches the Second Segment (Drops off).

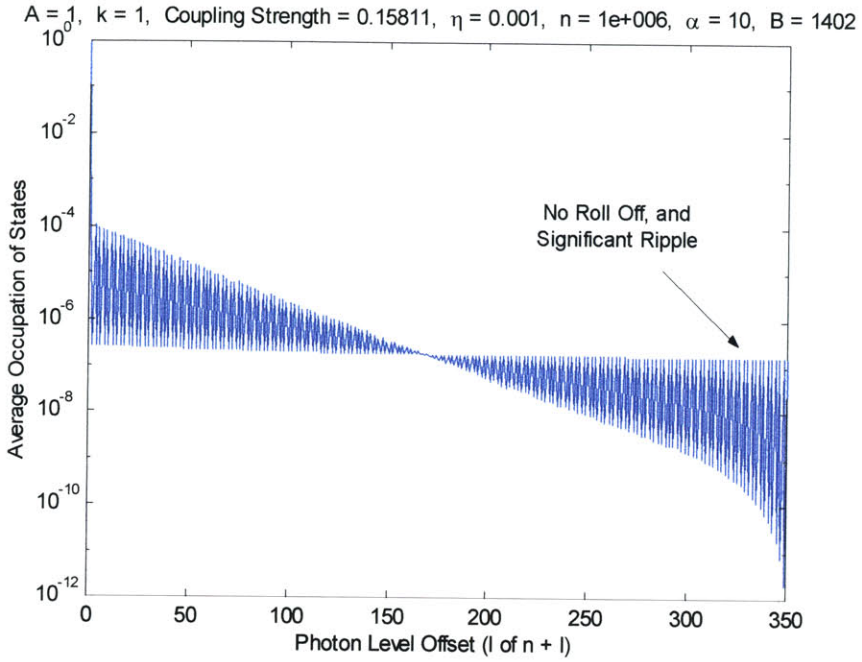

Figure 9: System IV—Significant Ripple, and no Apparent Roll Off

Table 3: Period Variation over Photon Level

System Periods Versus l							
System I		System II		System III		System IV	
l	Period	l	Period	l	Period	l	Period
5	1.726	10	$1.824 \cdot 10^8$	25	$1.819 \cdot 10^7$	20	$8.6 \cdot 10^7$
20	1.724	25	$1.823 \cdot 10^8$	50	$1.824 \cdot 10^7$	50	$1.72 \cdot 10^7$
35	1.724	40	$1.821 \cdot 10^8$	100	$1.817 \cdot 10^7$	100	$4.3 \cdot 10^6$
50	1.724	75	$1.816 \cdot 10^8$	250	$1.815 \cdot 10^7$	200	$1.6 \cdot 10^7$
				350	$1.815 \cdot 10^7$		

Chapter 5

RESULTS I

The number of atoms, A; the coupling strength, g; the photon level of the oscillator, n; and the ratio of energy between the systems (off-resonant ratio), η, affect the way the energy of the system evolves. Note that these parameters are normalized versions of our model:[1]

$$\eta = \frac{\hbar\omega}{\Delta E} \tag{5.1}$$

$$g = \frac{V}{\Delta E} \tag{5.2}$$

The normalized Hamiltonian is then

$$\hat{H}_n \equiv \frac{\hat{H}}{\Delta E} = \frac{\hat{\Sigma}_z^A}{2} + \frac{\hat{\Sigma}_z^B}{2} + \eta\hat{a}^\dagger\hat{a} + g\left(\hat{a} + \hat{a}^\dagger\right)^k\left(\hat{\Sigma}_x^A + \hat{\Sigma}_x^B\right) \tag{5.3}$$

We anticipate clear trends in the dynamics of the system that are analytic functions of these four parameters—A, g, n, and η. For example, the stronger the coupling, g, the shorter we would expect the period of energy transfer between cavities to be, because the coupling pathway between cavities is more easily crossed. Similarly, as the number of atoms in a cavity increase, the Dicke coherence factors increase. The stronger the coherence factors the stronger the interaction between cavities, i.e. the effective coupling. Therefore,

[1] This definition for g is different from the standard g that Hagelstein uses in his papers.

we expect the periods to get smaller as A grows. Furthermore, when all atoms do interact coherently, we expect the rate of energy transfer to increase, because more atoms are transferring energy. Conversely, we expect that the more off-resonant the system and/or the higher the photon level, the larger the transfer period. These parameters are fundamental to the way the system operates; therefore, our results depend heavily upon the value of these parameters.

An analytic function that describes the period of transfer for this system is potentially very complicated. We would like to form a relation where each parameter's effect on the period is independent of all other parameters; or in mathematical terms, a separable function.

$$T(A,g,n,\eta) = f_A(A)\cdot f_g(g)\cdot f_n(n)\cdot f_\eta(\eta) \tag{5.4}$$

More realistically, the relation would include cross terms. For example,

$$f_{Ag}(A\cdot g), f_{An}(A\cdot n), f_{A\eta}(A\cdot \eta), f_{gn}(g\cdot n), f_{g\eta}(g\cdot \eta), \cdots \tag{5.5}$$

and

$$f_{Agn}(A\cdot g\cdot n), f_{Ag\eta}(A\cdot g\cdot \eta), \cdots \tag{5.6}$$

Also, it might include any higher order variants

$$f_{A^2gn}(A^2\cdot g\cdot n), f_{Ag^2n}(A\cdot g^2\cdot n), \cdots \tag{5.7}$$

To specify the answer exactly would be very complex, if possible. Therefore, this analysis empirically fits the curve with a low order approximation. The sources of error associated with this simplification are addressed subsequently.

One Atom in Each Cavity

Let us begin by setting up the system with one atom in each cavity. This eliminates any direct interaction between atoms, such as spin state cancellation (singlet and triplet states). In addition, all changes of state are completely coherent (all atoms in a cavity transition between their two excitation levels simultaneously).[1] With the number of Atoms, A, equal to one, the Dicke number, S, by equation (2.11) is

$$S = \frac{A}{2} = \frac{1}{2} \tag{5.8}$$

Shape of One-Atom Curve

An elementary problem analyzed in Quantum Mechanics is two coupled two-level systems. We know that the energy probability of this system oscillates between the two-level systems sinusoidally. In our model, one atom in each cavity is essentially two two-level systems coupled together with a slightly more involved coupling pathway. Therefore, we expect the shape of the one-atom curve to be similar to the Rabi oscillations of the simple case: sinusoidal. Figure 10 shows a typical one-atom curve with a red sinusoid superposed at the same frequency and amplitude. Notice the similarity between the blue and red curves. As we suspected, the typical one-atom case is sinusoidal.

A model with two identical two-level systems has only four possible states; therefore, it has four energy eigenvalues. Since both systems are identical with identical coupling each way, there are only two possible system frequencies: $|E_1 - E_2| = |E_2 - E_3| = \omega_0$ and $|E_1 - E_3| = 2\omega_0$. Our system, on the other hand,

[1] However, note that the de-excitation is far from enhanced, because there is no coherent advantage given by only one atom.

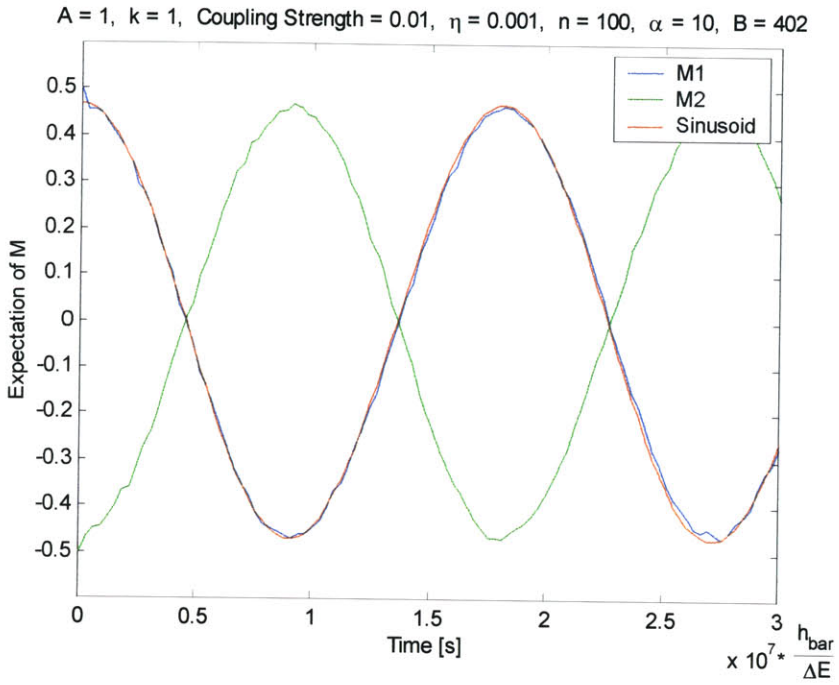

Figure 10: Typical One-Atom Energy Transfer Curve with Red Sinusoid Superposed

couples via an oscillator; this adds an infinite number of states. Therefore, our system may have ripple and unclear periods when two system frequencies with significant amplitude are close in value. The high frequency ripple specifically make slope measurements difficult and inaccurate. However, since the shape is fundamentally sinusoidal, we may extract the slope of the line by integrating.

$$M(t) = C\sin\left(\frac{2\pi}{T}t\right) \tag{5.9}$$

$$M'(t) = 2\pi\frac{C}{T}\cdot\cos\left(\frac{2\pi}{T}t\right) \tag{5.10}$$

Therefore, the maximum slope is 2π times the amplitude over the period:[1]

$$\text{Max slope} = 2\pi\frac{C}{T} \tag{5.11}$$

Parameter Trends

The coupling strength, photon level, and off-resonance affect the dynamics of the system. We have mapped out the periods and slopes over reasonable ranges for these parameters; the exhaustive results are in Appendix E. However, each parameter section includes a table extracted from Appendix E highlighting its respective trends.

Coupling strength, g

At the start of this chapter, we argued on physical grounds that the period would decrease as the coupling increased. Assuming this argument is true, we can argue that the maximum slope will increase by equation (5.11). Table 4 and Figure 11 show that the data agree with our reasoning; the period changes inversely with g and the maximum slope, proportionally.

On the log-log plot of Figure 11, the period has a slope of negative two, therefore, the system is inversely proportional to g^2.

$$\frac{\text{Period}}{\hbar/\Delta E} \equiv T \propto \begin{cases} \dfrac{1}{g^2} & g < 0.1 \\ \dfrac{1}{g} & g > 0.1 \end{cases} \tag{5.12}$$

[1] This formula does not hold for energy transfers that do not look sinusoidal, for example when two frequencies that are close together both have significant amplitudes.

The maximum slope, on the other hand, increases with a slope of one giving a proportional dependence of g.

$$\frac{\text{Max Slope}}{\Delta E/\hbar} \equiv m_x \propto \begin{cases} g^2 & g < 0.1 \\ g & g > 0.1 \end{cases} \tag{5.13}$$

As we would expect from equation (5.11) the period and maximum slope mirror each other; therefore, the dynamics for the one-atom case remain sinusoidal for changing g.

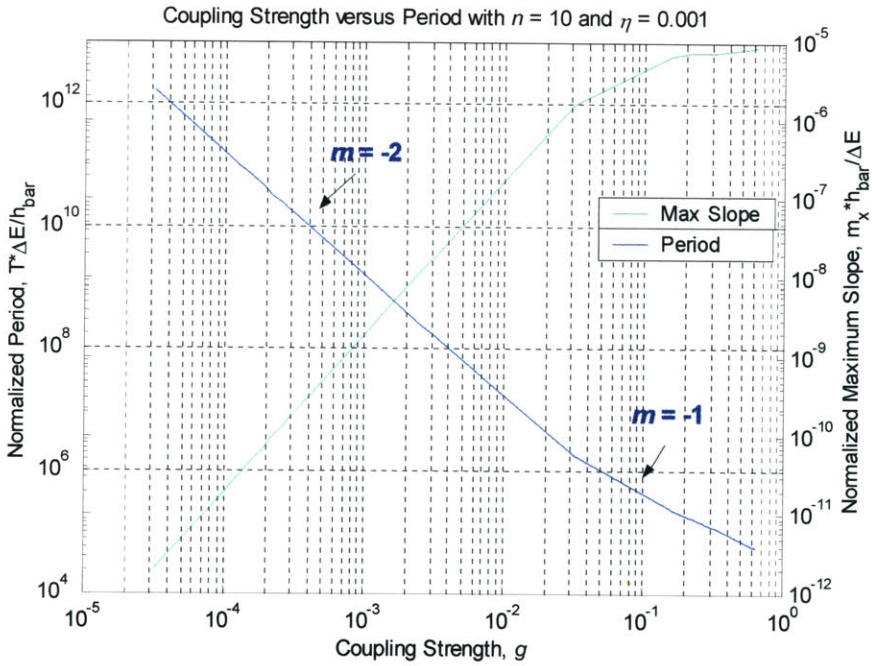

Figure 11: Period and Maximum Slope of Energy Transfer v/s g (n = 10, η = 0.001)

Table 4: Period and Maximum Slope of Energy Transfer v/s g (n and η fixed)

n	g	η	Max Slope $\cdot \frac{\hbar}{\Delta E}$	T $\cdot \frac{\Delta E}{\hbar}$
10	3.1623E-05	0.001	1.9970E-12	1.5730E+12
10	6.3246E-05	0.001	7.9538E-12	3.9300E+11
10	9.4868E-05	0.001	1.7860E-11	1.7400E+11
10	1.2649E-04	0.001	3.1806E-11	9.8400E+10
10	1.5811E-04	0.001	4.9927E-11	6.3000E+10
10	1.8974E-04	0.001	7.1611E-11	4.3700E+10
10	2.2136E-04	0.001	9.7906E-11	3.1000E+10
10	2.5298E-04	0.001	1.2722E-10	2.4600E+10
10	2.8460E-04	0.001	1.6117E-10	1.9400E+10
10	3.1623E-04	0.001	1.9945E-10	1.5700E+10
10	9.4868E-04	0.001	1.79E-09	1.7500E+09
10	1.5811E-03	0.001	4.9908E-09	6.2950E+08
10	2.5298E-03	0.001	1.2647E-08	2.4650E+08
10	3.1623E-03	0.001	1.9931E-08	1.5700E+08
10	3.1623E-02	0.001	1.6449E-06	1.8250E+06
10	1.5811E-01	0.001	6.8693E-06	2.3700E+05
10	2.2136E-01	0.001	7.5000E-06	1.7600E+05
10	3.1623E-01	0.001	7.6952E-06	1.2000E+05
10	6.3246E-01	0.001	8.5000E-06	5.7000E+04

Photon Level, n

We have suggested that the period will increase as the photon level increases, and therefore, the maximum slope will decrease. Table 5 and Figure 12 show that the period is proportional to n, and the slope inversely proportional. Specifically, at high n, the period grows as its square root; at low n, the period is unaffected.

$$T \propto \begin{cases} \sqrt{n} & n > 100 \\ 1 & n < 100 \end{cases} \tag{5.14}$$

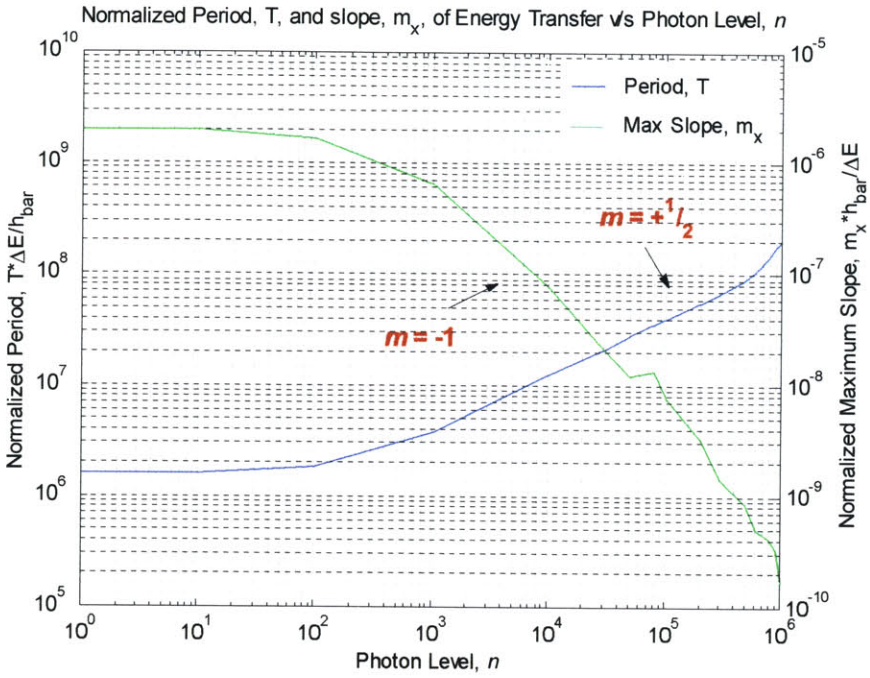

Figure 12: Period and Maximum Slope of Energy Transfer v/s n ($g = 0.01$, $\eta = 0.01$)

Table 5: Period and Maximum Slope of Energy Transfer v/s n (g and η fixed)

n	g	η	Max Slope $\cdot \frac{\hbar}{\Delta E}$	T $\cdot \frac{\Delta E}{\hbar}$
1	0.01	0.01	1.9915E-06	1.5800E+06
10	0.01	0.01	1.9549E-06	1.6000E+06
100	0.01	0.01	1.6597E-06	1.8200E+06
1000	0.01	0.01	6.5264E-07	3.6700E+06
10000	0.01	0.01	7.7500E-08	1.2400E+07
30000	0.01	0.01	2.1500E-08	2.1000E+07
50000	0.01	0.01	1.2000E-08	2.8000E+07
80000	0.01	0.01	1.3362E-08	3.5710E+07
100000	0.01	0.01	7.8570E-09	3.9000E+07
200000	0.01	0.01	3.2660E-09	5.5000E+07
300000	0.01	0.01	1.4290E-09	6.7000E+07
500000	0.01	0.01	8.3333E-10	9.3000E+07
600000	0.01	0.01	5.0000E-10	1.0700E+08
800000	0.01	0.01	4.1667E-10	1.4500E+08
900000	0.01	0.01	3.3333E-10	1.8000E+08
1000000	0.01	0.01	1.6667E-10	2.0000E+08

The maximum slope has a similar trend, it is constant at low n, and inversely proportional at large n.

$$m_x \propto \begin{cases} \frac{1}{n} & n > 100 \\ 1 & n < 100 \end{cases} \tag{5.15}$$

This trend differs from what we expect. The maximum slope and period do not inversely track each other; therefore, it suggests that the transfer curve is not strictly sinusoidal. Figure 13 shows a curve in the high n regime and the transfer is still clearly sinusoidal; however, the amplitude is very low. The low amplitude of the transfer curve causes the discrepancy in the maximum slope. Equation

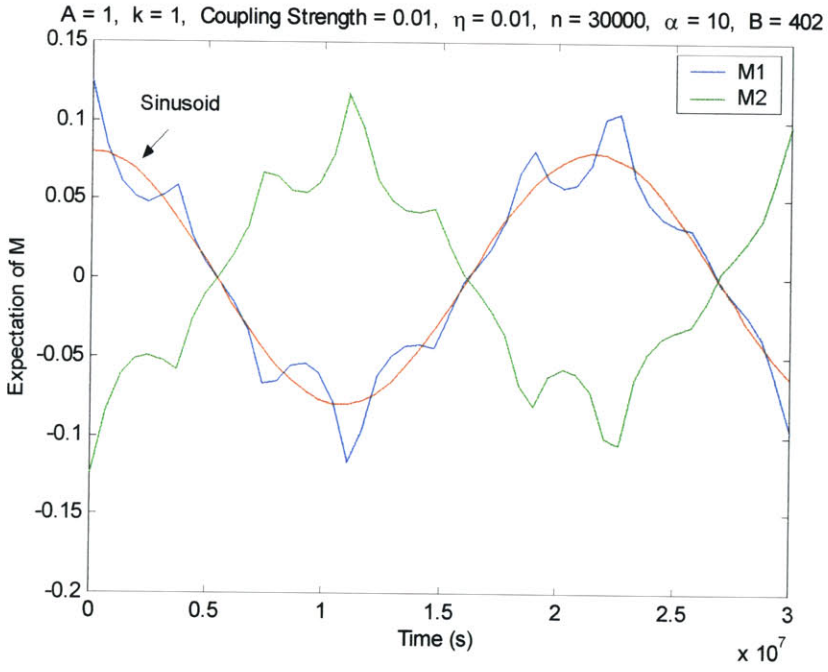

Figure 13: Energy Transfer Curve for High n Regime. Still Sinusoidal

(5.11) shows a direct dependence of the maximum slope on the amplitude of the sinusoid. The amplitudes of most curves have been very similar with a value around 0.5; therefore, their periods and maximum slopes track inversely proportionally. The curve in Figure 13 is less than one fifth of the norm (~0.08). In the high n regime, the amplitude is no longer constant but decreases with n; therefore, this extra variable gives a discrepancy in the symmetry between the maximum slope and period.

Off-Resonant Energy Ratio, η

Fixing g and n and varying η shows a simple dependence on the off-resonance.

$$T \propto \frac{1}{\eta} \tag{5.16}$$

$$m_x \propto \eta \tag{5.17}$$

The maximum slope and period trends in η clearly have a sinusoidal relationship. See Figure 14 and Table 6 below.

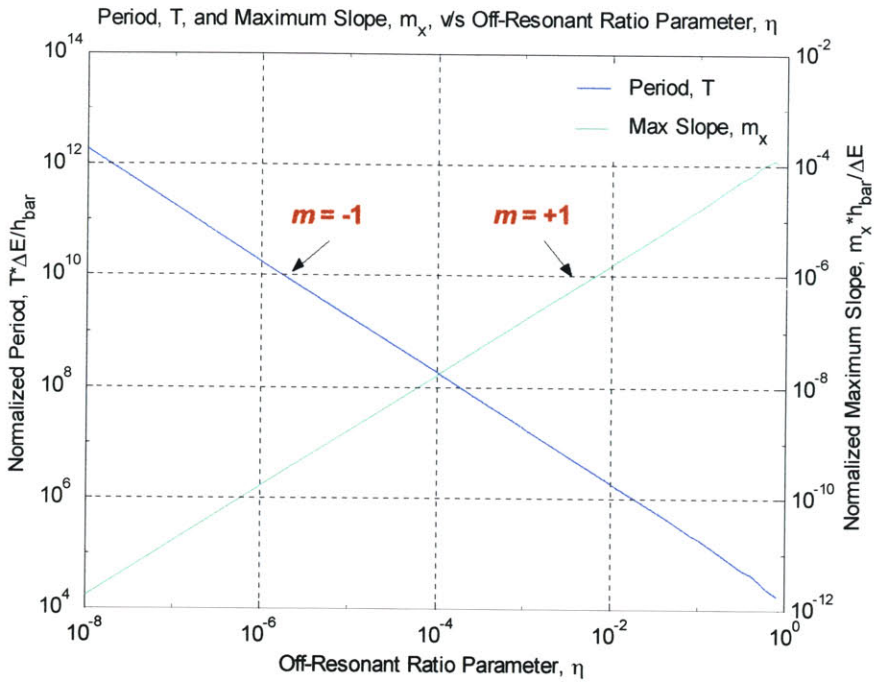

Figure 14: Period and Maximum Slope of Energy Transfer v/s η ($g = 0.01$, $n = 100$)

Table 6: Period and Maximum Slope of Energy Transfer v/s η (g and n fixed)

n	g	η	Max Slope $\cdot \frac{\hbar}{\Delta E}$	T $\cdot \frac{\Delta E}{\hbar}$
100	0.01	1.00E-08	1.6596E-12	1.8200E+12
100	0.01	0.000001	1.6596E-10	1.8200E+10
100	0.01	0.0001	1.6596E-08	1.8200E+08
100	0.01	0.001	1.6596E-07	1.8200E+07
100	0.01	0.01	1.6597E-06	1.8200E+06
100	0.01	0.05	8.3108E-06	3.6300E+05
100	0.01	0.08	1.3329E-05	2.2600E+05
100	0.01	0.1	1.6697E-05	1.8100E+05
100	0.01	0.2	3.4161E-05	8.8000E+04
100	0.01	0.3	5.3709E-05	5.5400E+04
100	0.01	0.4	6.8190E-05	4.2900E+04
100	0.01	0.5	9.4014E-05	3.1100E+04
100	0.01	0.6	1.1142E-04	2.4000E+04
100	0.01	0.7	1.2395E-04	1.9700E+04
100	0.01	0.8	1.1667E-04	1.7200E+04

Analytic Representation of Period and Maximum Slope

Combining the parameter's lower-value regimes from the above results gives a very simple relation for the normalized period and slope.

$$T = 18.2\frac{\sqrt{n}}{g\eta} \tag{5.18}$$

$$m_x = \frac{2\pi}{T}\beta = 2\pi\frac{g\eta}{\sqrt{n}}\beta \tag{5.19}$$

The maximum slope takes advantage of the sinusoidal shape of the transfer as described earlier. β is the average peak amplitude of the system. Ideally, $\beta = 0.5$ if all of the energy transfers between the systems; however, we use a more realistic choice of $\beta = 0.47$. Note, as we have seen earlier, the use of a constant for β will not work in the large n limit. These rough empirical estimates work surprisingly well. This particular result is under the columns marked "Simple I" in the Appendix E. Notice how well these estimates predict the dynamics in the low η, and low $g\sqrt{n}$ ranges.

We can improve our estimate by including the breakpoints in the above data for g and n. The new expressions are

$$T = \frac{\pi}{2}\frac{\left[\left(\frac{n}{200}\right)^2 + 1\right]^{\frac{1}{4}}\left[\left(\frac{g}{0.04}\right)^2 + 1\right]^{\frac{1}{2}}}{g^2\eta} \tag{5.20}$$

$$m_x = \frac{2\pi}{T}\beta = 4\beta \frac{g^2\eta}{\left[\left(\frac{n}{200}\right)^2 + 1\right]^{\frac{1}{4}}\left[\left(\frac{g}{0.04}\right)^2 + 1\right]^{\frac{1}{2}}} \tag{5.21}$$

These estimates are also in Appendix E under the columns marked "Simple II".

The simple relations above do well in very confined ranges; however, they are only useful for a general understanding of the dynamic dependence. To accurately specify the dynamics beforehand, more advanced modeling is necessary. We have improved the above estimates significantly by using bode-plot analysis. We fix all variables but one, and plot its progression on a log-log plot. Every change in slope can be modeled by a multiplicative pole or zero. Since the system is in three dimensions and we are empirically fitting it in one dimension at a time, there are undoubtedly errors associated with the results. Specifically, the particular value of a parameter at which a change in slope occurs (breakpoint) will be a function of the other two parameters. Our break points are not functions of the other two parameters, but we have compensated for it by averaging them over a reasonable range. Our final result is marked in Appendix E as "Advanced II". Equations (5.22) and (5.23) are the analytic formulas (with normalization constants) and Figure 15, Figure 16, and Figure 17 show plots of the actual curves next to the predicted curves.

$$T = \frac{\hbar}{\Delta E}\cdot\frac{1.62}{g^2\eta}\cdot\left[1+\left(\frac{g\sqrt{n}}{0.1}\right)^2\right]^{\frac{1}{4}}\cdot\left[1+\left(g\sqrt{n}\right)^2\right]^{\frac{1}{2}}\cdot\left[1-\left(\frac{\eta}{1.225}\right)^2\right]^{\frac{1}{2}} \tag{5.22}$$

$$m_x = \frac{\Delta E}{\hbar}\cdot\frac{2\pi\beta}{1.62}\cdot\frac{g^2\eta}{\left[1+\left(\frac{g\sqrt{n}}{0.1}\right)^2\right]^{\frac{1}{4}}\cdot\left[1+\left(g\sqrt{n}\right)^2\right]^{\frac{1}{2}}\cdot\left[1-\left(\frac{\eta}{1.225}\right)^2\right]^{\frac{1}{2}}} \tag{5.23}$$

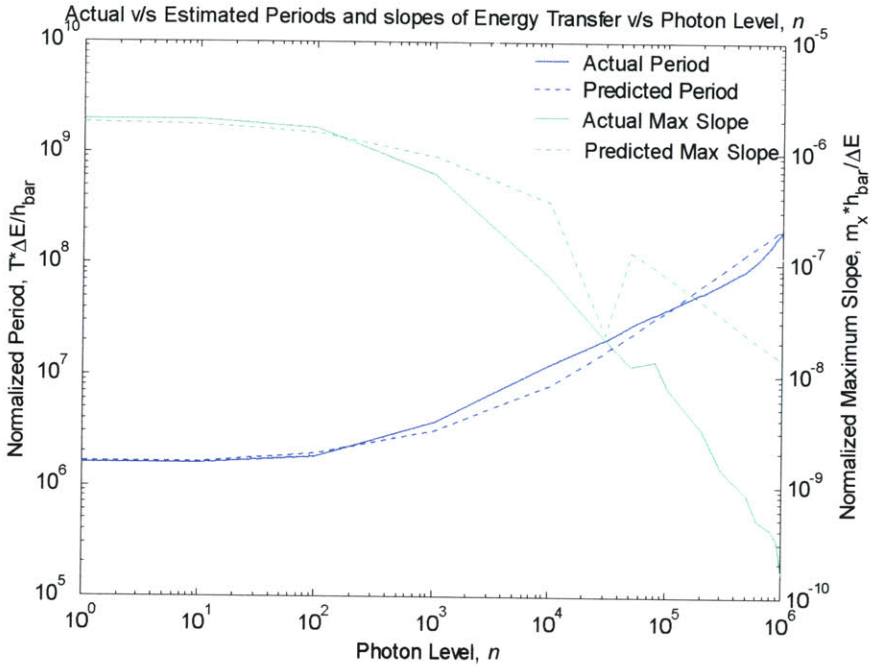

Figure 16: Actual Period and Maximum Slopes versus Estimated Values over Photon number n

$(g = 0.01,\ \eta = 0.01)$

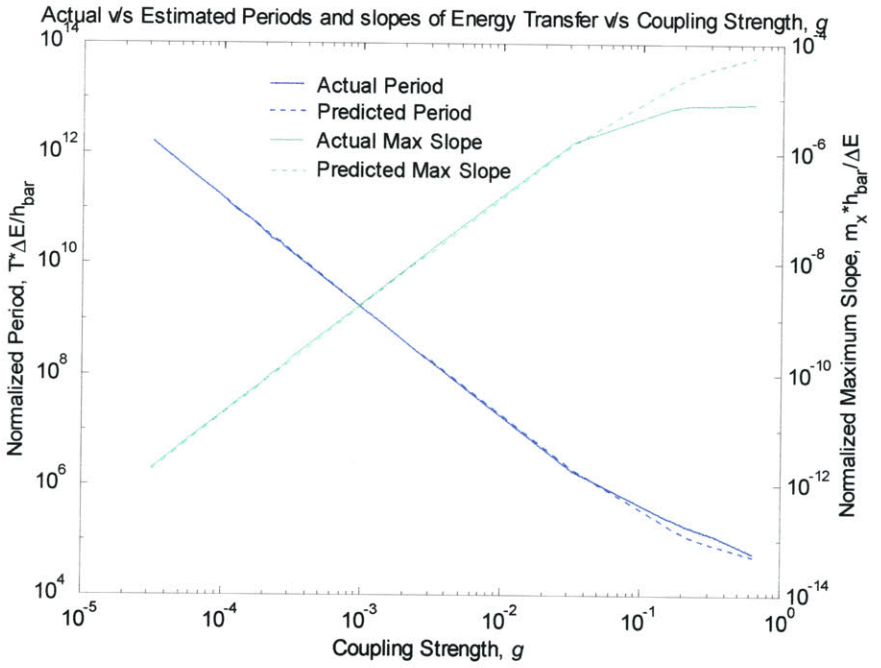

Figure 15: Actual Period and Maximum Slopes versus Estimated Values over Coupling Strength g

$(n = 10,\ \eta = 0.001)$

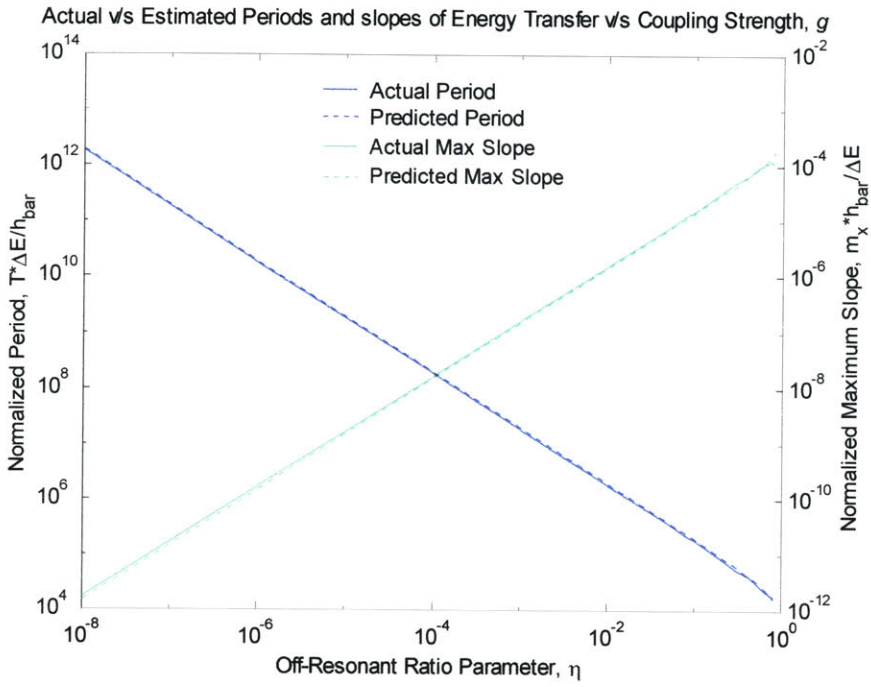

Figure 17: Actual Period and Maximum Slopes versus Estimated Values over Coupling Strength g $(n = 10,\ \eta = 0.001)$

Notice that the maximum slope error in Figure 15 is due to the variation of the amplitude. There are small errors in the period and rate for large g and n, this is the strong coupling limit. All other points follow very closely.

Three Atoms in Each Cavity

The lowest A where we anticipate non-linearity in the curves is the three-atom case. In both the one-atom case and the two-atom case, the M-coefficients have the same magnitude: $\frac{1}{2}$ and 1, respectively. The three-atom case however, can be $\frac{1}{2}$ or $\frac{3}{2}$; therefore, we anticipate non-linearity in the probability of energy

transfer. Specifically, we expect the slope to increase, and in the large A-limit, we expect the sinusoid to approach a square wave.

Figure 18 shows a typical three-atom energy transfer curve with a red sinusoid superimposed. The curve is non-linear; however, another eigenvalue is giving significant disturbance to the transfer. It is difficult to discern if the curve has higher transfer rates than the one-atom case, or whether the higher slopes are indicative of the extra perturbation.

Appendix F includes a table that lists the periods and slopes for the three-atom experiment. Comparing the three-atom periods to the one-atom periods, show that they remain essentially constant. The three-atom periods are only about 3%

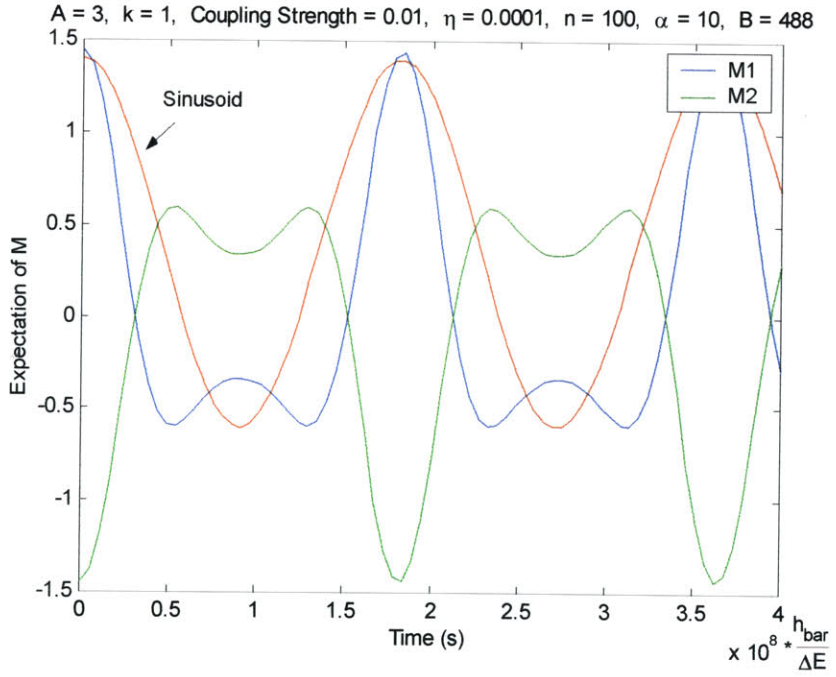

Figure 18: 3-Atom Energy Transfer Curve, Illustrating Non-Linearity from Sinusoid

less than the one-atom periods. Conversely, there is a big change between the slopes of the two systems. The slope increases by a factor of roughly three to four from that of the one-atom case (the rate-increase factor is a range because the extra perturbation described above contributes error to the slope calculation).

Many Atoms in Each Cavity

Computation resources limit our ability to explore higher atom cases, because our basis must include enough states so that the photon level boundaries have negligible state occupation. In a real implementation of this system, the basis is infinite, and the only true boundary for photon level is $n = 0$; therefore, for four or more atomic systems, the necessary finite basis becomes enormous. The Gaussian initialization approach is not sufficient to examine higher cases (without significant increase in computer power). We must look for a different approach. The next chapter examines another method of initialization that is fundamentally stronger, and that allows us to partially circumvent the computational limitation.

Let us first graphically describe what we expect for many-atom systems. As discussed in the three-atom system, we expect that the transfer curves become non-linear as A increases, due to the increase in possible coefficients. This increase in the Dicke enhancement factor physically represents an increase in coherent interaction; therefore, we expect the slope of the transfer to increase. Figure 19 illustrates our predictions.

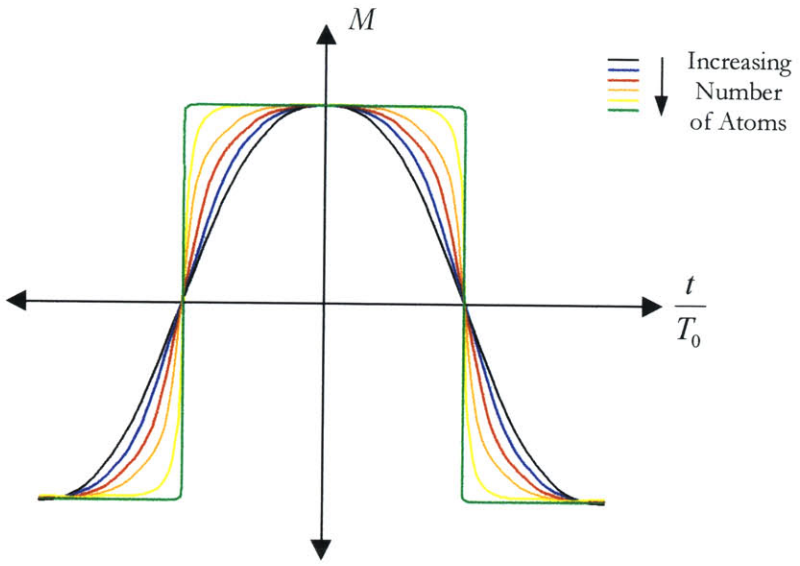

Figure 19: Prediction of Transfer Curve for Increasing Number Of Atoms

Chapter 6

GENERALIZED COHERENT STATES

Chapter 3 examines a couple of ways to improve the dynamic model of the system by optimizing the initial state. The goal of the optimization is to maximize the coherent transfer between cavity A and cavity B. The results in Chapter 5 use the Gaussian initialization defined at the end of Chapter 3. This method improves the visibility of the periods of energy transfer over the single-state initialization proposed at first; however, more enhancement is needed. Ideally, the coefficients are chosen so that the probability-of-energy-transfer curve between the two states of interest yields maximum transfer and minimum distortion.

Ideally, we want the energy to transfer between cavity A and cavity B classically (coherently). The picture described in Chapter 3 under the Gaussian initialization section describes essentially a **generalized coherent state**. However, while the Gaussian approach estimates the initial energies well, it is far from a coherent state. To initialize in a coherent state, we need to approach the problem from a different angle.

In a SHO, placing the system in a coherent state is straightforward; the wave packet must follow a classical trajectory, and its size must remain constant. To initialize a SHO in a classical state, we would localize the wave packet at the center of motion with maximum velocity. Our system is much more complex than a SHO, but we may use a similar strategy. Picture a pendulum swinging, its maximum velocity occurs when its potential energy is at a minimum (at the center

of motion). To place our system in a coherent state, it should be localized near $\langle M_B - M_A \rangle = 0$, with maximum velocity. This Chapter attempts to use the initial conditions to place the system into a quasi-coherent state.

Initialization

Maximization of Energy Transfer Velocity

We define a new operator that focuses on the relative energy of the cavities.

$$\hat{Q} = \hat{\Sigma}_z^B - \hat{\Sigma}_z^A \tag{6.1}$$

The expectation of operator $\langle \hat{Q} \rangle$ describes the transfer of energy between the two cavities; it is a position operator for the energy. To achieve maximum coherent transfer, we want to maximize the velocity of energy transfer; therefore, the change in $\langle \hat{Q} \rangle$ must be at a maximum.

$$\text{Maximize: } \frac{d}{dt}\langle \hat{Q} \rangle \tag{6.2}$$

The Ehrenfest equation allows us to remove the derivative in equation (6.2) and form a relation from the Hamiltonian:

$$\frac{d}{dt}\langle \hat{Q} \rangle = \frac{1}{i\hbar}\langle [\hat{Q}, \hat{H}] \rangle \tag{6.3}$$

For clarity, let $\hat{K}$ be the velocity operator

$$\hat{K} = \frac{1}{i\hbar}[\hat{Q}, \hat{H}] \tag{6.4}$$

If an initial state, ψ_j, is chosen such that the normalized expectation of $\hat{K}$ is maximized, then the transfer of energy between the cavities is also maximized.

$$\text{Maximize: } \frac{\langle\psi|\hat{K}|\psi\rangle}{\langle\psi|\psi\rangle} \tag{6.5}$$

The ψ_j that maximizes equation (6.5) is an eigenvector of $\hat{K}$.

$$\hat{K}\psi = \lambda\psi \tag{6.6}$$

Localization of Wave Packet

To create a generalized coherent state, further constraints are necessary. We must localize the wave packet and place it in the center of motion (for symmetry). Centering the packet requires two conditions

$$\frac{\langle\psi|\hat{Q}|\psi\rangle}{\langle\psi|\psi\rangle} = 0 \tag{6.7}$$

$$\frac{\langle\psi|\hat{l}|\psi\rangle}{\langle\psi|\psi\rangle} = 0 \tag{6.8}$$

where

$$\hat{l} = \hat{n} - n_0 \tag{6.9}$$

Localization around the center requires two more conditions. The wave packet must have room to oscillate. If the packet is too small, the dynamics are dominated by dispersion; however, if it is too large, the energy is no longer

localized. We suspect that the system has some ideal spread; however, it is not clear what that value is. For the cases with small numbers of atoms, we assume that the spread in $\hat{Q}$ and $\hat{l}$ should be as large as possible without reaching the boundaries of the finite basis.

$$\Delta Q^2 < \mathrm{Max}(Q) \tag{6.10}$$

$$\Delta l^2 < \mathrm{Max}(Q) \tag{6.11}$$

In Figure 20, we outline an ideal initial state for our basis over two dimensions, l v/s Q. As we increase the size of the basis, the $l-$**height** increases; however, for a given number of atoms, A, the Q-**width** is fixed. We add two constraints to equation (6.6):

$$\hat{K}\psi = \lambda\psi + \lambda'\hat{Q}\psi + \lambda''\hat{l}\psi \tag{6.12}$$

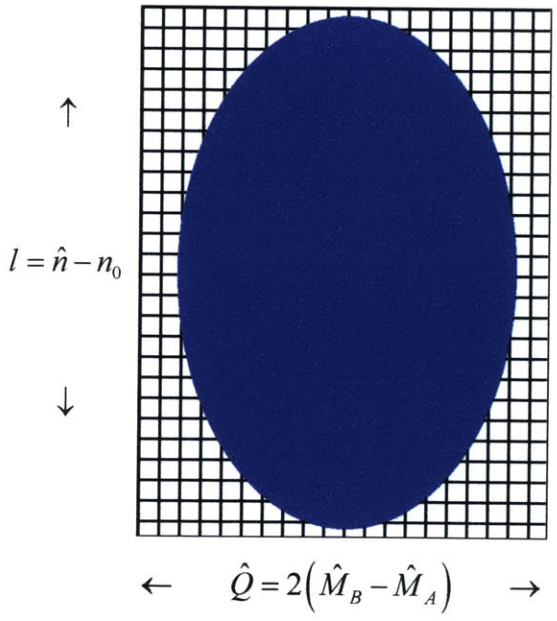

Figure 20: Ideal Localization for Initial State in l and Q

By varying λ' and λ'', we control the spread of $\langle \hat{Q} \rangle$ and $\langle \hat{I} \rangle$ independently.

Implementation

Derivation of $\hat{K}$

Combining equations (2.1), (6.1), and (6.4) yield

$$\hat{K} = \frac{1}{i\hbar}\left[\hat{Q}, \hat{H}\right] = \frac{1}{i\hbar}\left[\left(\hat{\Sigma}_z^B - \hat{\Sigma}_z^A\right), \begin{pmatrix} \frac{\Delta E}{2}\left(\hat{\Sigma}_z^A + \hat{\Sigma}_z^B\right) + \hbar\omega_0 \hat{a}^\dagger \hat{a} \\ +V\left(\hat{a} + \hat{a}^\dagger\right)^k \left(\hat{\Sigma}_x^A + \hat{\Sigma}_x^B\right) \end{pmatrix}\right] \tag{6.13}$$

Deleting the terms that commute, leaves

$$\begin{aligned} \hat{K} &= \frac{1}{i\hbar}\left[\hat{Q}, \hat{H}\right] = \frac{1}{i\hbar} V\left(\hat{a} + \hat{a}^\dagger\right)^k \left(\left[\hat{\Sigma}_z^B, \hat{\Sigma}_x^B\right] - \left[\hat{\Sigma}_z^A, \hat{\Sigma}_x^A\right]\right) \\ &= \frac{V\left(\hat{a} + \hat{a}^\dagger\right)^k}{i\hbar}\left(2i \cdot \hat{\Sigma}_y^B - 2i \cdot \hat{\Sigma}_y^A\right) = \frac{2V\left(\hat{a} + \hat{a}^\dagger\right)^k}{\hbar}\left(\hat{\Sigma}_y^B - \hat{\Sigma}_y^A\right) \end{aligned} \tag{6.14}$$

Therefore

$$\hat{K} = \frac{2V\left(\hat{a} + \hat{a}^\dagger\right)^k}{\hbar}\left(\hat{\Sigma}_y^B - \hat{\Sigma}_y^A\right) \tag{6.15}$$

$\hat{K}$ is analogous to the $\hat{v}$ of an SHO. This is beautiful! It is a clean representation of velocity for our system, which we can use to generate temporary coherent states for a rather complex system. This powerful approach allows us to monitor a very complex system almost trivially.

Implementation of Velocity Operator

Rewriting equation (6.12) with the operators on one side gives

$$\hat{K}_{\text{Constrained}}\psi = \left(\hat{K} - \lambda'\hat{Q} - \lambda''\hat{l}\right)\psi = \lambda\psi \tag{6.16}$$

Combining equations (6.1), (6.15), and (6.16) yield

$$\left[\frac{2V\left(\hat{a}+\hat{a}^{\dagger}\right)^{k}}{\hbar}\left(\hat{\Sigma}_{y}^{B}-\hat{\Sigma}_{y}^{A}\right)-\lambda'\left(\hat{\Sigma}_{z}^{B}-\hat{\Sigma}_{z}^{A}\right)-\lambda''\left(\hat{\alpha}^{\dagger}\hat{a}-n_{0}\right)\right]\psi=\lambda\psi \tag{6.17}$$

Σ_y is imaginary; so, equation (6.17) is not Hermitian. This means that the eigenvalues are complex. The imaginary part corresponds to the velocity, and the real part to the position.

One of the eigenvectors of equation (6.17) contains a suitable initial condition. To determine which eigenvector is appropriate, we must examine the localization and velocity of each. There are six useful parameters to monitor: $\langle\hat{Q}\rangle$, $\langle\hat{l}\rangle$, ΔQ^2, Δl^2, $\langle\hat{K}\rangle$, and $\Delta\varepsilon^2$.

$$\begin{aligned}
&\langle\hat{Q}\rangle \approx 0\\
&\langle\hat{l}\rangle \approx 0\\
&\Delta Q \rightarrow \text{Adjustable}\\
&\Delta l \rightarrow \text{Adjustable}\\
&\langle K\rangle = \text{Maximum}\\
&\Delta\varepsilon \approx ?
\end{aligned} \tag{6.18}$$

Again, we do not yet know the appropriate spread values for large A and l; however, for small values, we maximize the spread without hitting the boundaries. Continuing this research to higher number of atoms require much more powerful computational power and coding systems quicker than Matlab. Once this research is continued, we hope to find appropriate targets for the spreads.

Applying equation (6.15) to the basis gives a velocity matrix, $\overline{\overline{K}}$. $\overline{\overline{K}}$ is completely off-diagonal, because $\hat{K}$ only contains raising or lowering operators. However, when we add the constraints from equation (6.12), $\overline{\overline{K}}_{Constrained}$ has diagonal values. Appendix C, *Table Generator*, includes a program that determines $\langle \hat{Q} \rangle$, $\langle \hat{l} \rangle$, ΔQ^2, Δl^2, $\langle \hat{K} \rangle$, $\langle \hat{K}^2 \rangle$, and $\Delta \varepsilon^2$ for all of the eigenvectors. From these values, we can choose an appropriate initial condition and begin the system in a coherent state.

Chapter 7

RESULTS II

Results II uses the generalized coherent state initialization technique described in the previous chapter to predict energy dynamics. We have established that the generalized coherent state is a powerful approach mathematically; however, the true strength of a method lies in its ability to generate considerable transfer of energy between the two cavities. Therefore, our first task is to prove that this method works, second, that it is reliable (consistent with our earlier calculations), and most importantly, that we can use it to predict the dynamics of cases with larger A.

Functionality and Reliability of Generalized Coherent State Initialization

Let us take a simple case where $n = 100$, $g = 0.01$, and $\eta = 10^{-4}$, and compare the responses between the Gaussian initialization and the generalized coherent state initialization. Figure 21 shows a one-atom energy transfer curve initialized with a generalized coherent state. Again, we have superimposed a perfect sinusoidal function in red (identical to the Gaussian case, see Figure 10), so that the correlation is clear. The period and slope are identical to the curve initialized with Gaussian elimination. There is some ripple on the curve; however, this choice of initialization generates transfer of energy between system A and B, and its dynamics match that of the known data in chapter 5, Results I.

Figure 22 shows a second example with three atoms. This graph shows a slight nonlinearity between the sinusoidal motion and the three-atom transfer;

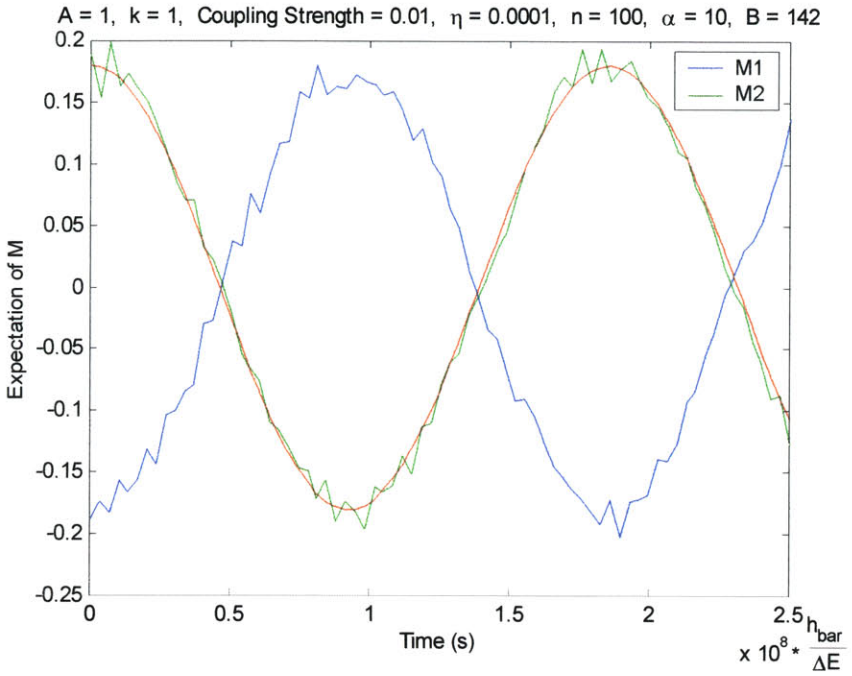

Figure 21: 1-Atom Energy Transfer Curve with Generalized Coherent State Initialization

specifically, the slope seems to be larger. However, this aberration is far from marked. Comparing Figure 18 with Figure 22 immediately shows an advantage gained by the generalized coherent state approach. The frequency components that were not filtered by the Gaussian approach make its response difficult to ascertain slope, while the generalized coherent state method eliminates this ambiguity clearly illustrating how slight (if at all) the non-linearity is.

We have shown that we can generate the desired dynamic response with a generalized coherent state approach. However, care must be taken in choosing the appropriate initialization eigenvector. Just as in the Gaussian venue, if states on the photon boundary have significant occupation level, the response is dominated by the artificial boundary. This typically increases the frequency of the response. The program, PositionMap, in Appendix D graphically depicts the occupation level on a ΔM versus l plot. This is useful in determining whether

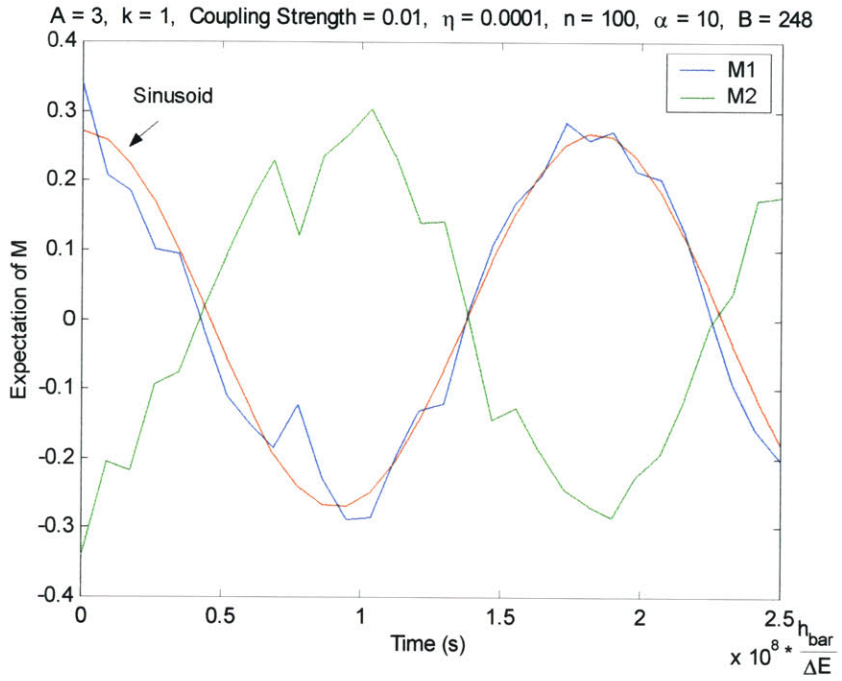

Figure 22: 3-Atom Energy Transfer Curve with Generalized Coherent State Initialization

or not a particular choice of initialization eigenvector accurately represents the system.

Increasing the Number of Atoms, A, with the Generalized Coherent State Approach

The generalized coherent state method lends itself more versatility. Since, we must keep the occupation away from the photon boundaries, the Gaussian approach is limited to very small A because of finite computational resources. However, the generalized coherent state method has two controls that constrain the size of the basis necessary: λ' and λ''. λ' restricts the spread in ΔM, while λ'' limits the spread in photon number. Therefore, we can analyze systems with larger A by constraining the spread of the initial occupation. However, since this is a generalized coherent state, the system will fall out of coherence, and possibly

spread to the boundaries. The program, PositionMap, described above may also be used to determine the validity of the solution over time.

Figure 23 shows a 4-atom case using the generalized coherent state method to limit the span in photon levels. The photon spread is limited to $l = 24$, which corresponds to 613 states. With this few photon levels, the Gaussian elimination method results would not be very accurate. However, for the generalized coherent state method, we seem to have accurate results. The period is the same as it was in the three-atom and one-atom case, this agrees with the trend and our intuition. The slope is not clear because of an aberration in the curve similar to the three-atom case using Gaussian filtering; however, the speed of transfer is clearly increased from that of the three-atom case.

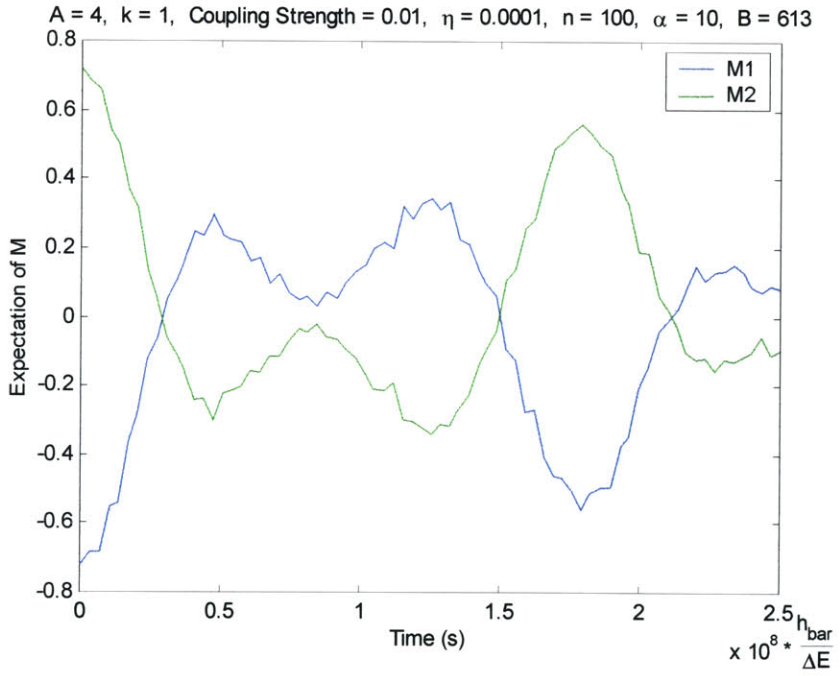

Figure 23: 4-Atom Energy Transfer Curve with Generalized Coherent State Initialization

Examining the second period of the curve in Figure 23 shows a change in dynamics. The peaks are loosing magnitude, for the first peak begins at 0.7 while the second peak only reaches 0.5; similarly, the first valley reaches -0.3, while the in the second cycle it only reaches -0.1. This seems to be the coherent state falling apart, for the transfer is not as great so the coherence factors must be decreasing.

Chapter 8

SCALING VERSUS COUPLING STRENGTH

The coupling strength is fundamental to our system. If there is no coupling, the system is relatively uninteresting; and the stronger the coupling, the more complex the system dynamics are. We have previously labeled g as the coupling strength of the system and we have defined it in equation (5.2) (repeated here for convenience) as the normalized, coupling parameter, V, of the Hamiltonian.

$$g = \frac{V}{\Delta E} \tag{8.1}$$

However, our representation of the coupling strength is not indicative of the actual coupling between states. Specifically, with the present g, the system can be in a strong coupling regime with small g; and similarly, in a weak coupling regime with large g. This chapter examines this underlying parameter and redefines it such that it more accurately describes the system's true coupling.

Stationary Development of New Coupling Parameter

Peter Hagelstein has investigated extensively the stationary eigenvalues of our system. In his studies, he has used a slightly modified definition for g. He defines the coupling parameter to represent the normalized strength of coupling between any two states. Specifically

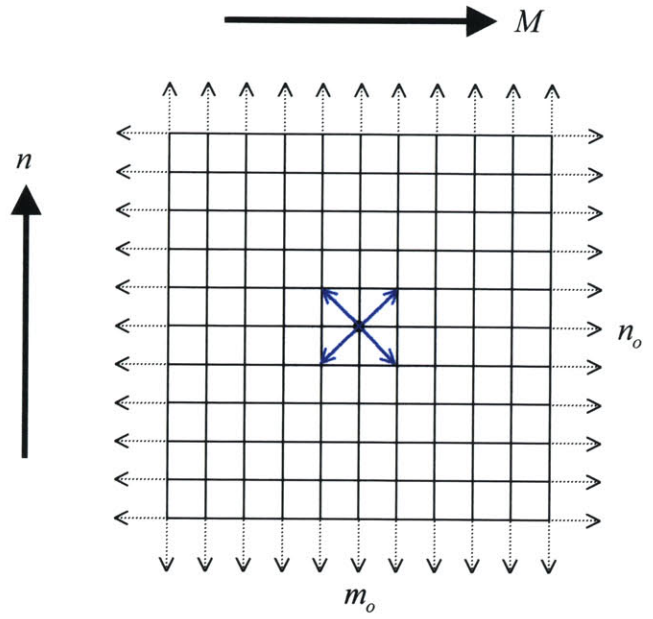

Figure 24: Diagram of Generic Large System with Coupling Pathways Outlined for One State: m_o, n_o

$$g = \left| \frac{\langle i | H | f \rangle}{\Delta E} \right|_{m_o, n_o} \tag{8.2}$$

Where i represents the initial state, and f, the final state. m_o and n_o are the initial state's M and n values. See Figure 24. With this definition, the four coupling pathways outlined in Figure 24 would be:

$$g = \begin{cases} \frac{V}{\Delta E}\sqrt{n_0+1}\sqrt{S(S+1)-m_0(m_0+1)} \\ \frac{V}{\Delta E}\sqrt{n_0+1}\sqrt{S(S+1)-m_0(m_0-1)} \\ \frac{V}{\Delta E}\sqrt{n_0}\sqrt{S(S+1)-m_0(m_0+1)} \\ \frac{V}{\Delta E}\sqrt{n_0}\sqrt{S(S+1)-m_0(m_0-1)} \end{cases} \tag{8.3}$$

For relatively large m_0 and n_0, g simplifies to

$$g \approx \frac{V}{\Delta E}\sqrt{n_0}\sqrt{S^2 - m_0^2} \tag{8.4}$$

while this is relatively simple to handle for stationary cases, it varies for our dynamic system.

Dynamic Development of New Coupling Parameter

The definition in equation (8.4) is dependent upon M. For a stationary system, M remains constant, and this definition is a simple and accurate representation of the coupling. However, for a dynamic system, the intent of the dynamics is to shift M (defined as $M_2 - M_1$) from $-2S$ to $2S$. This means that g is a function of time.

For a one-atom case, the weighting by M is constant—1; therefore, g can only equal $\frac{V}{\Delta E}\sqrt{n}$. This means that $g_{\min_1} = g_{\max_1} = \frac{V}{\Delta E}\sqrt{n}$. The two-atom case is similar in that there is only one weighting term due to M: $\sqrt{2}$. Therefore, $g_{\min_2} = g_{\max_2} = \sqrt{2}\frac{V}{\Delta E}\sqrt{n}$. However, for $A \geq 3$, the weighting varies according to position in M. The three-atom case is the first system with differing values of g.

$$\begin{aligned} g_{\min_3} &= \sqrt{3}\frac{V}{\Delta E}\sqrt{n} \\ g_{\max_3} &= 2\frac{V}{\Delta E}\sqrt{n} \end{aligned} \tag{8.5}$$

The period is defined by the edges—the length of time to shift from M equals $-2S$ to M equals $2S$. In this region, g is at a minimum. On the other hand, the maximum rate of transfer is defined in the middle, when $M = 0$. g is maximum in the middle. Therefore, it makes sense to scale the period in terms of $g_{\min}$, and the rate in terms of $g_{\max}$.

We feel that this revised definition for the coupling parameter, g, is more accurate and fundamental to the system. The remainder of this chapter reexamines the results of Chapters 5 and 7 with the new g. The results clearly show the system's dependence on this parameter.

Scaling of Rate with New Coupling Parameter

The rate for the one atom case was determined in Chapter 5. It is

$$m_x = \frac{\Delta E}{\hbar} \cdot \frac{2\pi\beta}{1.62} \cdot \frac{g^2\eta}{\left[1+\left(\frac{g\sqrt{n}}{0.1}\right)^2\right]^{\frac{1}{4}} \cdot \left[1+\left(g\sqrt{n}\right)^2\right]^{\frac{1}{2}} \cdot \left[1-\left(\frac{\eta}{1.225}\right)^2\right]^{\frac{1}{2}}} \tag{8.6}$$

As suggested above, the analytic dependence has already shown an effective g of $g\sqrt{n}$. We can rearrange the above rate into a polynomial (adjusted to improve matching with constant β)[1]

[1] As discussed previously, β is a function of coupling also. When the coupling is strong $(\tilde{g} > 0.1)$, β decreases from the ideal of 0.5. At $g \approx 1$, there is a marked drop in the amplitude, which significantly reduces the rate (although not the period). Since β varies according to the coupling, we can empirically model it within the coupling polynomial, and set $\beta = 0.5$. This is what accounts for the change in the new rate equation.

$$m_x = \frac{\Delta E}{\hbar} \cdot \frac{\pi}{1.62} \cdot \frac{g^2 \eta}{\left[1 + 25\left(g\sqrt{n}\right)^2 + 0.444\left(g\sqrt{n}\right)^4\right] \cdot \left[1 - \frac{\eta^2}{1.9}\right]^{\frac{1}{2}}} \tag{8.7}$$

Now if we rewrite this relation with the new effective coupling parameter, $\tilde{g}$, (which for the one-atom case is $\tilde{g} = g\sqrt{n}$) we get

$$\gamma \equiv m_x = \frac{\Delta E}{\hbar} \cdot \frac{\pi}{1.62} \cdot \frac{\frac{\tilde{g}^2 \eta}{n}}{\left[1 + 25\tilde{g}^2 + 0.444\tilde{g}^4\right] \cdot \left[1 - \frac{\eta^2}{1.9}\right]^{\frac{1}{2}}} \tag{8.8}$$

If we look at the rate with respect to $\tilde{g}$, we expect a clear transition from weak coupling to strong coupling. Figure 25 shows the actual rate and the empirical formula for rate versus the new coupling parameter, $\tilde{g}$; the rates shown are with $A = 1$, $n = 10$, and $\eta = 0.001$ (however, the general formula above holds for any n and η; we do not have enough data points to claim that it holds for any number of atoms, A). The empirical estimation and the simulation results match closely. Notice that the largest rates are around $g \approx 1$, this is the strong coupling regime. The rates decrease for smaller or larger g.

We may generalize our rate formula above by creating a constant (in g) that includes all constants and function of n and η,

$$\gamma_0 = \frac{\Delta E}{\hbar} \cdot \frac{\pi}{1.62} \cdot \frac{1}{n} \cdot \frac{\eta}{\left(1 - \frac{\eta^2}{1.9}\right)^{\frac{1}{2}}} \tag{8.9}$$

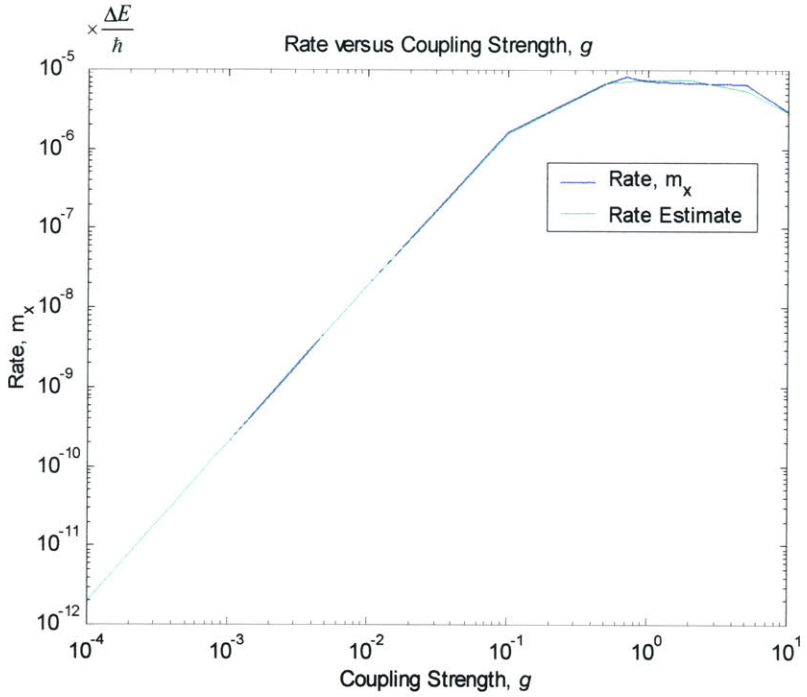

Figure 25: Rate versus Coupling Strength (effective g)

This yields a general formula for the transfer rate as a function of the coupling parameter g

$$\gamma = \gamma_0(n,\eta)\cdot\frac{\tilde{g}^2}{1+25\tilde{g}^2+0.444\tilde{g}^4} \tag{8.10}$$

Chapter 9

CONCLUSION

This thesis examined the dynamics of energy exchange in a model for second-order (indirect) coupling through off-resonant states. We have shown that the model hosts a second-order transfer of energy between two collections of two level systems via an off-resonant oscillator. We have also addressed some of the difficulties associated with this novel type of transfer, namely that the frequencies of the oscillator and two-level systems are different. We have illustrated measurable coupling through coherent enhancement analogous to Dicke's superradiance.

We have also characterized the period and rate of energy-transfer between the isolated systems, and have shown patterns that analytically depend upon the number of atoms in each cavity, the coupling strength, the photon level, and the off-resonant ratio parameter. Furthermore, this characterization uses dimensionless quantities and therefore is applicable to many different disciplines.

Our key result is the normalized rate of energy transfer for a general system

$$\gamma = \gamma_0(n,\eta)\cdot\frac{\tilde{g}^2}{1+25\tilde{g}^2+0.444\tilde{g}^4} \tag{9.1}$$

Research Issues

There is much area for continuation of this research. The atomic patterns are estimated theoretically, and have only been supported by a few data points. Furthermore, the large atom limits are of particular interest because they allow for large Dicke enhancement; so, we need more powerful computational power (and more efficient compiled code) to work out solutions to the model with many atoms. We have characterized the model with Matlab 5.3, this proves to be very slow, and memory intensive for $A > 3$, or for highly off-resonant/low photon regimes. The appendices include the code that we used in calculating the above model. The rate equation, should be characterized for large A, and checked for accuracy in the large g regime.

The approach of initializing the system as a generalized coherent state is the most powerful feature of this thesis; however, it is still largely an intellectual one. Further research is needed to understand the issues that we found that separate our model from the intuition gained from a generalized coherent state. Once these issues are understood, we may attack an arbitrary problem in this model more quickly and effectively. The generalized coherent state is a very powerful approach to this problem and problems like this in general and should be used in future research.

APPENDICES

A. Dynamics—Evolution of System via Matlab Code
B. Hamiltonian Generator—Generation of Hamiltonian with Matlab Code
C. Coherent Constraints—Coefficient and Table Generators in Matlab Code
D. PositionMap—Three Dimensional Representation of State Occupation through Matlab Code
E. One-Atom Energy Oscillation Periods v/s Parameters
F. Three-Atom Energy Oscillation Periods v/s Parameters

Appendix A: Dynamics—Evolution of System via Matlab

```
function [M,u,t,H,v,E,Basis, E_K, c_K,K,MaxSlope,SlopeIndex] = Dynamics(A,k,B,t_max,n,g,eta,Points,alpha,lambda1,lambda2,State1)
% This program mathematically evolves the  quantum system.  It allows
%     three choices for state initialization (and more can be systematically
%     added):
%
%     1.  Single State Initialization
%         This scheme automatically chooses state |s,s⟩_A |s,-s⟩_B |n_0⟩
%         as the initial state.  No other parameters are necessary
%
%     2.  Gaussian Filtered Eigenvalues Initialization
%         The initial state is determined by a Gaussian weighting of
%         the eigenvalues.  Specify alpha, typically 10 is a good value.
%         c = exp(-alpha*(E-Ec)^2)
%
%     3.  Generalized Coherent State Initialization
%         This approach is more advanced; however, it requires more
%         interaction.  Both lambda1 (the M-constraint) and lambda2
%         (the n-constraint) must be set.  Also, the appropriate eigenstate
%         to crunch must be specified, state1 (the programs tablegen and
%         positionmap will be helpful in determining which one to choose).
%
%
%     The program flowmap is as follows:
%
%     1.  Setup Basis and create Hamiltonian (handled by HamGen)
%     2.  Find Eigenvalues and Eigenfunctions (H * v_k = E_k * v_k).
%     3.  Specify initial conditions (coherent initialization invokes
%         CoGen to determine coefficients)
%     4.  u_m(t) = sum_k(conj(v_k_INITIAL) * exp(i*E_k*t/h_bar) * v_k,m).
%     5.  Plot M1 and M2 (The time averaged occupations of each system
%         (A and B) summed over all n).  Plot Photon Contribution across
%         l, the photon distance from n_0.
%


% Specify Initialization Approach by uncommenting the appropriate choice.
Initial_Type = 'Gaussian';
%Initial_Type = 'Coherent';
%Initial_Type = 'SingleSt';



% Specify which plots to plot
PhotonPlot = 'True'; %'Fals'; %
DynamicsPlot = 'True'; %'Fals'; %
```

Appendix A: Dynamics—Evolution of System via Matlab

```
% If Progress Report is true, the computer provides text feedback
%   for the progression of the simulation.  Very helpful for long sims.
ProgressReport = 'True'; %'Fals'; %


% Specify the start and finish states.  Recommended leaving as 1 and B.
Start = 1; %B/2;
Finish = B; %B/2+1;


Quantum;    %Sets up variables for h_bar, etc.

% Initialize Matrix values
ga = g;
gb = ga;

Params = [n,ga,gb,eta];



%=========================================================================
% Generate Basis, Hamiltonian and find eigenvalues and eigenfunctions.

[H,E,v,l,l_final,Basis] = HamGen(A, k, B, Params);
if ProgressReport == 'True', disp('Hamiltonian Generated'), end;

% Convert the Diagonal matrix of energy eigenvalues to a vector
Temp = E;
E = zeros(B,1);
for i_count = 1:B
   E(i_count) = Temp(i_count,i_count);
end


%=========================================================================
% Setup Initial Conditions (Coefficients)

u_init = zeros(B,1);

switch Initial_Type
   case 'Coherent'
      [K,E_K,c_K] = CoGen(Basis, A, k, Params, lambda1, lambda2);

      % Need some way to determine which state to use as initial.
```

Appendix A: Dynamics—Evolution of System via Matlab

```
        state_count = State1;
        u_init = c_K(:,state_count);

    case 'Gaussian'
        u_init(1) = 1;

        % Calculates mean energy (the extra code converts from diagonal to normal)
        E_Target = mean(E);
        a = alpha;

    case 'SingleSt'
        u_init(1) = 1;
end


%=========================================================================
% Calculate Dynamics

t = linspace(0, t_max, Points);

% Setup Normalization Constant
Norm = 0;
for k_count = 1:B
    switch Initial_Type
    case 'Coherent'
        Norm = Norm + abs(v(:,k_count)'*u_init)^2;
    case 'Gaussian'
        Norm = Norm + abs(v(:,k_count)'*u_init)^2 * exp(-2*a*(E(k_count) - E_Target)^2);
    case 'SingleSt'
        Norm = Norm + abs(v(:,k_count)'*u_init)^2;
    end
end
Norm = sqrt(Norm);

u = sparse(zeros(B,length(t)));

% NEW Variable M1 & M2 that focuses on final/initial state occupation, ignoring osc. level
M = sparse(zeros(2,length(t)));


for m = Start:Finish %1:B
    for k_count = 1:B
        switch Initial_Type
        case 'Coherent'
```

Appendix A: Dynamics—Evolution of System via Matlab

```
            % The u_init specifies a coherent state for the system to begin in.
            u(m,:) = u(m,:) + (v(:,k_count)'*u_init * exp(-i*E(k_count)*t) * v(m,k_count))/Norm;
        case 'Gaussian'
            % Adds a gaussian scaling to an initial state placement (l).
            u(m,:) = u(m,:) + (v(:,k_count)'*u_init * exp(-a*(E(k_count)-E_Target)^2) * exp(-i*E(k_count)*t) * v(m,k_count))/Norm;
        case 'SingleSt'
            % Simple initialization of energy in state specified by u_init
            u(m,:) = u(m,:) + (v(:,k_count)'*u_init * exp(-i*E(k_count)*t) * v(m,k_count))/Norm;
        end
    end

    if ProgressReport == 'True', disp(m), end;
end


M(1,:) = Basis(:,1)'*abs(u).^2;
M(2,:) = Basis(:,2)'*abs(u).^2;


% The following plots all of the occupations on one graph, still
%    available; however, cumbersome if greater than roughly 50 states.

%if DynamicsPlot == 'True'
%    Plot the results and format graph
%    figure(1);
%    plot(t,abs(u).^2);
%    title(sprintf('A = %0.5g,  k = %0.5g,  Coupling Strength = %0.5g,  \\eta = %0.5g,  n = %0.5g,  \\alpha = %0.5g,  B = %0.5g', A, k, g,
eta, n, a, B));
%    xlabel('Time (s)');
%    ylabel('Occupation of States');
    %ax = axis;
%    axis([0 t_max -0.1 1.1]);

%    leg = [];
%    for m = 1:B
%        if and(m ~= l, m ~= l_final)
%            legt = sprintf('State %d', m);
%        elseif m == l
%            legt = sprintf('Init State %d', m);
%        elseif m == l_final
%            legt = sprintf('Final State %d', m);
%        end
%        leg = [leg, {legt}];
%    end
%    legend(leg,-0);
%end
```

Appendix A: Dynamics—Evolution of System via Matlab

```
if PhotonPlot == 'True'
   % Look at probabilities v/s photon level, where N = n + l
   L = Basis(1,3);
   State = 1;
   for i_count = L:-1:-L
      PhotonTemp = 0;

      if Basis(State, 3) == i_count
         StillOnPhotonLevel = 1;
      else
         StillOnPhotonLevel = 0;
      end

      while StillOnPhotonLevel == 1
         PhotonTemp = PhotonTemp + abs(u(State,:)).^2;
         State = State + 1;
         if State > B
            StillOnPhotonLevel = 0;
         elseif Basis(State, 3) ~= i_count
            StillOnPhotonLevel = 0;
         end
      end

      Photon(i_count+L+1) = mean(PhotonTemp);
   end
   figure(2);
   semilogy(0:L,Photon(L+1:2*L+1));

   title(sprintf('A = %0.5g,  k = %0.5g,  Coupling Strength = %0.5g,  \\eta = %0.5g,  n = %0.5g,  \\alpha = %0.5g,  B = %0.5g', A, k, g,
                 eta, n, alpha, B));
   xlabel('Photon Level Offset (l of n + l)');
   ylabel('Average Occupation of States');

end
figure(3);
plot(t,M);
title(sprintf('A = %0.5g,  k = %0.5g,  Coupling Strength = %0.5g,  \\eta = %0.5g,  n = %0.5g,  \\alpha = %0.5g,  B = %0.5g', A, k, g, eta,
              n, alpha, B));
xlabel('Time (s)');
ylabel('Expectation of M');

leg = [{sprintf('%s','M1')}, {sprintf('%s','M2')}];
legend(leg,1);
```

Appendix A: Dynamics—Evolution of System via Matlab

```
% If desired, the graphs can be saved from within Dynamics.
if 1 == 0
   FileName = sprintf('eigen_%d', state_count);
   saveas(1, FileName, 'fig');
   FileName2 = sprintf('Photon_%s', FileName);
   saveas(2, FileName2, 'fig');
   FileName = sprintf('M_%s', FileName);
   saveas(3, FileName, 'fig');
end  %if 1==0
```

Appendix B: Hamiltonian Generator—Generation of Hamiltonian with Matlab

```
function [H,E,c,l_init,l_final,Basis] = HamGen(A, k, B, Params)
% Hamiltonian = HamGen(A, k, B, Params)
%
%    HamGen returns a numerical Hamiltonan with the Params supplied.  This
%       can not be done symbolically because of the eigenvalue function.
%
%       A       The number of atoms
%       k       The order of photon exchange
%       B       The total number of states (this code should be converted to l input)
%       Params  Array of Parameters for Hamiltonian, Params = [n, ga, gb, e];
%
%                n:  The number of photons
%               ga:  The coupling Strength between SHO and System A normalized by two-level system resonant energy
%               gb:  The coupling strength between SHO and System B normalized by two-level system resonant energy
%                e:  The ratio of Energy between Two-Level System and Oscillator.  E_osc = e * E_2-level
%
%
% [Hamiltonian, Energy ,Eigenvector, l_init, l_final, Basis] = HamGen(A, k, B, Params)
%
%    Returns the Hamiltonian, Energy eigenvalues, Eigenvectors, initial and
%       final states of M assuming n = n0, and the Basis of form [M1,M2,n-n0].
%
%


% From the number of states, B, and the number of Atoms, A, determine size of basis
%    and various constants.
TotalAtomStates = (A+1)^2;
switch mod(k,2)
case 1
   StatesOnInitLevel = ceil(TotalAtomStates/2);
   StatesOnAdjacentLevel = floor(TotalAtomStates/2);
   % The last parameter adds the first set of intermittent states parallel to the initial and
   %      and final states.  This simplifies the code to work from the center out, instead of
   %      adding all states from one run, and then second, etc.
   MinimumNumberOfStates = StatesOnInitLevel + 2*StatesOnAdjacentLevel + (k-1)*TotalAtomStates;
case 0
   StatesOnInitLevel = TotalAtomStates;
   StatesOnAdjacentLevel = 0;
   MinimumNumberOfStates = StatesOnInitLevel * (k + 1);
end

% Error Check-Determines if B is correct given number of Atoms
ErrorMessage = sprintf('\nIncorrect Number of States. \n     For %d atoms, B must equal:  \n\n          B = %d + a*%d + b*%d \n\n     Where
                       ''a'' can be any non-negative integer, and ''b'' can equal either 0 or 1\n     Note: B must be at least %d',
                       A,StatesOnInitLevel,2*TotalAtomStates,2*StatesOnAdjacentLevel,MinimumNumberOfStates);
```

Appendix B: Hamiltonian Generator—Generation of Hamiltonian with Matlab

```
if B >= MinimumNumberOfStates
   LeftOver = B - StatesOnInitLevel;

   switch mod(LeftOver, TotalAtomStates)
   case 0
      % Correct Number Of States to achieve a symmetric Hamiltonian
      % Total Photon Levels, L
      L = LeftOver / TotalAtomStates;
   case 2*StatesOnAdjacentLevel
      % Correct Number Of States to achieve a symmetric Hamiltonian
      % Total Photon Levels, L
      L = floor(LeftOver / TotalAtomStates) + 1;
   otherwise
      error(ErrorMessage);
   end

else
   error(ErrorMessage);
end


% All combinations of possible M1 and M2 are necessary.  They both
%     range from -S:+S.
S = A / 2;


% Extract Parameters from input
n = Params(1);
g(1) = Params(2);
g(2) = Params(3);
e = Params(4);


%=========================================================================
% Basis Generation
i = 1;
Basis = zeros(B,3);
for l = L:-1:-L
   j = 1;
   for M2 = -S:S
      for M1 = -S:S

         if CheckState(M1,M2,l,j,A,k) == 1
            Basis(i,:) = [M1,M2,l];
            if l == 0
               if and(M1 == S, M2 == -S), l_init = i; end;
```

Appendix B: Hamiltonian Generator—Generation of Hamiltonian with Matlab

```
            if and(M1 == -S, M2 == S), l_final = i; end;
        end;
        i = i+1;
    end
    j = j + 1;
  end
 end
end


%=========================================================================
% Create Hamiltonian Based off above Basis
H = zeros(B,B); %sparse(B,B);
for i = 1:B
   for j = i:B
      M1 = [Basis(i,1),Basis(j,1)];
      M2 = [Basis(i,2),Basis(j,2)];
      l = [Basis(i,3),Basis(j,3)];

      if i == j
         if n + l(1) <= 0, n_plus_l = 0; else, n_plus_l = n + l(1); end;
         %        2*M1*deltaE/2
         H(i,i) = 2*M1(1)*0.5 + 2*M2(1)*0.5 + e*n_plus_l;
      else
         % For a value other than zero, either M1 or M2 must be
         %    exactly one apart, and the other one, must be equal to zero.
         DeltaM = [M1(1)-M1(2);M2(1)-M2(2)];
         Deltal = l(1)-l(2);

         % The following if statement assures two things: 1. M1 or M2 transitions
         %     a value of one from 'j' to 'i', 2. The relative photon levels of 'j'
         %     and 'i' are exactly k or k-2 (This works for upto k = 3).
         if and(and(sum(abs(DeltaM)) == 1, prod(abs(DeltaM)) == 0),and(mod(abs(Deltal),2) == mod(k,2), abs(Deltal) <= k))
            % Cross Coefficient is the movement from state 'j' to state 'i'.
            %     Since, the atomic transitions have already been pinned to a
            %     delta of one, the values of 'j' can simply be plugged into
            %     the coefficient formula.  If 'j' moves up one to get to state
            %     'i', then the formula is M*(M+1); otherwise it is M*(M-1), since
            %     DeltaM defines if it moves up or down, it can be used as the +/- 1

            if DeltaM(1) == 0
               System = 2;
               M = M2(2);
            else
               System = 1;
               M = M1(2);
```

Appendix B: Hamiltonian Generator—Generation of Hamiltonian with Matlab

```
            end;

            T = sqrt(S*(S+1)-M*(M+DeltaM(System)));
            P = PhotonContribution(l(1),l(2),k,n);
            H(i,j) = T*g(System)*P;
         end
      end
   end
end;

% Fill in remaining values (Easy since Hermition Matrix).
H = H + (H - diag(ones(B,1)).*H)';

[c,E] = eig(H);



%%%%%%%%%%%%%%%%%%%%%%%%%%%%%%%%%%%%%%%%%%%%%%%%%%%%%%%%%%%%%%%%%%%%%%%%%%%%%%%
%%%%%%%%%%%%%%%%%%%%%%%%%%%%%%%%%%%%%%%%%%%%%%%%%%%%%%%%%%%%%%%%%%%%%%%%%%%%%%%

function CheckState = CheckState(M1,M2,l,Order,A,k)
% If the number of Atoms is odd, then the first possible case
%     |-M,-M> is in the adjacent photon level from the initial state.
Adjacent = mod(A,2);  %Equals 1 if Lowest State is in level with init state.

if mod(k,2) == 1
   % A pattern forms across the possible states of an atom such that every other
   %     state is in a different photon level.  However, it does not follow this
   %     strictly: every A+1 states alternates between the two adjacent photon
   %     levels; the states after every A+1 similarly alternate upto the next A+1
   %     state.  Therefore, 'a' determines two issues: 1. the distance of the state
   %     from its A+1 state, 2. whether or not that number is odd or even (same or
   %     different, respectively).  'b', on the other hand, determines which A+1
   %     state the state is in, and then also whether it is the same or different
   %     (odd or even).  This pattern is interesting only in the odd 'k' realm.
   a = mod(mod(Order-1,A+1) + 1, 2);
   b = mod(floor((Order-1)/(A+1)), 2);

   % Check if in initial photon level (or multiple of two).  The initial state is
   %     the last state of the first A+1 chain, and the first state of the last A+1
   %     chain.
   if mod(l,2) == 1
      if Adjacent == 0
         if mod((a + b), 2) == 0
            CheckState = 1;
         else
```

```
            CheckState = 0;
         end
      else
         if mod((a + b), 2) == 0
            CheckState = 0;
         else
            CheckState = 1;
         end
      end

   else  % If in adjacent photon level use the remaining states.

      if Adjacent == 0
         if mod((a + b), 2) == 0
            CheckState = 0;
         else
            CheckState = 1;
         end
      else
         if mod((a + b), 2) == 0
            CheckState = 1;
         else
            CheckState = 0;
         end
      end
   end
else
   % If k is not odd, than every possible state of the odd rows contribute
   %       to the system.
   CheckState = ~mod(l,2);
end


%%%%%%%%%%%%%%%%%%%%%%%%%%%%%%%%%%%%%%%%%%%%%%%%%%%%%%%%%%%%%%%%%%%%%%%%%%%%%%%%
%%%%%%%%%%%%%%%%%%%%%%%%%%%%%%%%%%%%%%%%%%%%%%%%%%%%%%%%%%%%%%%%%%%%%%%%%%%%%%%%

function P = PhotonContribution(l_final,l_init,k,n);
% l_final is the bra-state of the photon, and l_init is the ket-state.
%     l_init must transistion to l_final.

Deltal = l_final - l_init;

switch k
case 1
   switch Deltal
   case 1
```

Appendix B: Hamiltonian Generator—Generation of Hamiltonian with Matlab

```
        if n + l_init < 0
            P = 0;
        else
            P = sqrt(n + l_final);
        end
    case -1
        if n + l_init -1 < 0
            P = 0;
        else
            P = sqrt(n + l_init);
        end
    end
case 2
    switch Deltal
    case 2
        if n + l_init < 0
            P = 0;
        else
            P = sqrt(n + l_final)*sqrt(n + l_final - 1);
        end
    case 0
        if n + l_init - 1 < 0
            P = 0;
        else
            P = 2*(n+l_init) + 1;
        end
    case -2
        if n + l_init - 2 < 0
            P = 0;
        else
            P = sqrt(n + l_init)*sqrt(n + l_init - 1);
        end
    end
case 3
    switch Deltal
    case 3
        if n + l_init < 0
            P = 0;
        else
            P = sqrt(n + l_final)*sqrt(n + l_final - 1)*sqrt(n + l_final - 2);
        end
    case 1
        if n + l_init - 1 < 0
            P = 0;
        else
            P = 3 * (n + l_init + 1)^(3/2);
```

Appendix B: Hamiltonian Generator—Generation of Hamiltonian with Matlab

```
        end
    case -1
        if n + l_init - 2 < 0
            P = 0;
        else
            P = 3 * (n + l_init)^(3/2);
        end
    case -3
        if n + l_init - 3 < 0
            P = 0;
        else
            P = sqrt(n + l_init)*sqrt(n + l_init - 1)*sqrt(n + l_init -2);
        end
    otherwise
        error('Internal Code Problem with PhotonContribution')
    end
end
```

Appendix C: Coherent Constraints—Coefficient and Table Generators in Matlab

```
function [K_constrained,E,c] = Coefficient_Generator(Basis, A, k, Params, lambda1, lambda2)
% The function returns the matrix created by applying the
%    velocity operator with some conditions to the Basis passed
%    to it.  The result, is intended to produce localized states
%    with coherent energy transfer.  The velocity operator is
%
%    ^k/deltaE = 2*g/h_bar*(^a + ^a+)^k * (SIGMA_y^B - SIGMA_y^A)
%              = 2*g/h_bar*(^a + ^a+)^k * [S_+^B - S_-^B - S_+^a + S_-^a]/i
%
%    The constraints add localization.  There are two dimensions
%    to specify, and they are separable:  M and n
%
%    Total Operator:  <^K> - lambda'*<^Q> - lambda"*<^n-n_0>
%    Where: ^Q = (^SIGMA_z^B - ^SIGMA_z^A)
%
%    The equation to solve is
%
%          ^K |psi> = lambda |psi> + lambda'*^Q |psi> + lambda"*^n |psi>
%
%    combining the operators gives
%
%          (^K - lambda'*^Q - lambda"*^n) |psi> = lambda |psi>
%
% NOTE: ^K is imaginary (similar to a momentum operator...), and the eigenvalues
%       are real.  However, we need real values, so this program equivalently
%       calculates i*(^K...), which should give an imaginary eigenvalue and real
%       eigenvectors.
%
%
% Params is an array, that contains the parameters in the following order
%    Params = [n, ga, gb, e];
%
%      n:  The number of photons
%     ga:  The coupling Strength between SHO and System A
%     gb:  The coupling strength between SHO and System B
%      e:  The ratio of Energy between Two-Level System and Oscillator.  E_osc = e * E_2-level

Quantum;

% Extract Parameters from input
n = Params(1);
g(1) = Params(2);
g(2) = Params(3);
e = Params(4);

% All combinations of possible M1 and M2 are necessary.  They both
```

Appendix C: Coherent Constraints—Coefficient and Table Generators in Matlab

```
%     range from -S:+S.
S = A / 2;


% Create Operator Matrix from Basis
B = length(Basis);  %Using length on a 2D matrix, chooses the longest dimension

K_constrained = zeros(B,B);
for i_count = 1:B
   for j_count = i_count:B
      M1 = [Basis(i_count,1),Basis(j_count,1)];
      M2 = [Basis(i_count,2),Basis(j_count,2)];
      l = [Basis(i_count,3),Basis(j_count,3)];

      if i_count == j_count
         % Matrix element contribution from velocity operator is zero because the ^K always
         %     changes the state.  The contributions from ^Q and ^n do contribute.
         K_constrained(i_count,j_count) = -lambda1*(M2(2)-M1(2)) - lambda2*l(2);
      else
         % For the matrix element to have a value other than zero, either M1 or M2, but
         %    not both, must change by exactly one, the remaining parameter must not change.
         DeltaM = [M1(1)-M1(2);M2(1)-M2(2)];
         Deltal = l(1)-l(2);

         % The following if statement assures two things: 1. M1 or M2 transitions
         %     a value of one from 'j_count' to 'i_count', and 2. The relative photon levels of 'j_count'
         %     and 'i_count' are exactly k or k-2 (This works for upto k = 3).
         if and(and(sum(abs(DeltaM)) == 1, prod(abs(DeltaM)) == 0),and(mod(abs(Deltal),2) == mod(k,2), abs(Deltal) <= k))
            % Cross Coefficient is the movement from state 'j_count' to state 'i_count'.
            %     Since, the atomic transitions have already been pinned to a
            %     delta of one, the values of 'j_count' can simply be plugged into
            %     the coefficient formula.  If 'j_count' moves up one to get to state
            %     'i_count', then the formula is M*(M+1); otherwise it is M*(M-1), since
            %     DeltaM defines if it moves up or down, it can be used as the +/- 1

            if DeltaM(1) == 0
               System = 2;
               M = M2(2);
            else
               System = 1;
               M = M1(2);
            end;

            Sign = DeltaM(System);
            T = Sign/i * sqrt(S*(S+1)-M*(M+DeltaM(System)));  % See note in intro for the first 'i'
            P = PhotonContribution(l(1),l(2),k,n);
```

Appendix C: Coherent Constraints—Coefficient and Table Generators in Matlab

```
            K_constrained(i_count,j_count) = T*2*g(System)*P; %/h_bar
         end
      end
   end
end;

% Fill in remaining values (Easy since Hermition Matrix).
K_constrained = K_constrained + (K_constrained - diag(ones(B,1)).*K_constrained)';


[c,E] = eig(K_constrained);


%%%%%%%%%%%%%%%%%%%%%%%%%%%%%%%%%%%%%%%%%%%%%%%%%%%%%%%%%%%%%%%%%%%%%%%%%%%%%%%
%%%%%%%%%%%%%%%%%%%%%%%%%%%%%%%%%%%%%%%%%%%%%%%%%%%%%%%%%%%%%%%%%%%%%%%%%%%%%%%


function P = PhotonContribution(l_final,l_init,k,n);
% l_final is the bra-state of the photon, and l_init is the ket-state.
%      l_init must transistion to l_final.

Deltal = l_final - l_init;

switch k
case 1
   switch Deltal
   case 1
      if n + l_init < 0
         P = 0;
      else
         P = sqrt(n + l_final);
      end
   case -1
      if n + l_init -1 < 0
         P = 0;
      else
         P = sqrt(n + l_init);
      end
   end
case 2
   switch Deltal
   case 2
      if n + l_init < 0
         P = 0;
```

```
        else
            P = sqrt(n + l_final)*sqrt(n + l_final - 1);
        end
    case 0
        if n + l_init - 1 < 0
            P = 0;
        else
            P = 2*(n+l_init) + 1;
        end
    case -2
        if n + l_init - 2 < 0
            P = 0;
        else
            P = sqrt(n + l_init)*sqrt(n + l_init - 1);
        end
    end
case 3
    switch Deltal
    case 3
        if n + l_init < 0
            P = 0;
        else
            P = sqrt(n + l_final)*sqrt(n + l_final - 1)*sqrt(n + l_final - 2);
        end
    case 1
        if n + l_init - 1 < 0
            P = 0;
        else
            P = 3 * (n + l_init + 1)^(3/2);
        end
    case -1
        if n + l_init - 2 < 0
            P = 0;
        else
            P = 3 * (n + l_init)^(3/2);
        end
    case -3
        if n + l_init - 3 < 0
            P = 0;
        else
            P = sqrt(n + l_init)*sqrt(n + l_init - 1)*sqrt(n + l_init -2);
        end
    otherwise
        error('Internal Code Problem with PhotonContribution')
    end
end
```

Appendix C: Coherent Constraints—Coefficient and Table Generators in Matlab

```
function [delM_expect, deln_expect, del2_M, del2_n, expect_K, del2_E, del2_K2] = TableGen(Basis, K_constrained, c, E, A, H)
%
%  Takes a Basis and the state occupations, u, and map out the occupation
%       with respect to M2-M1 (Position) and n (photon number).
%
%  K_Constrained is the velocity matrix with position (M and n) constraints.
%       The equivalent pure velocity matrix is simply K_Contrained with zero
%       on the diagonals (see cogen.m)
%

%  B is the number of states
B = length(Basis);

K = K_constrained - diag(ones(B,1)).*K_constrained;


delM_expect = zeros(B,1);
deln_expect = zeros(B,1);
del_M2 = zeros(B,1);
del_n2 = zeros(B,1);
del2_M = zeros(B,1);
del2_n = zeros(B,1);
expect_K = zeros(B,1);
expect_K2 = zeros(B,1);
del2_E = zeros(B,1);
del2_K2 = zeros(B,1);


for eigen = 1:B
   M1 = Basis(:,1);
   M2 = Basis(:,2);
   l = Basis(:,3);

   OccProb = (abs(c(:,eigen))).^2;

   delM_expect(eigen) = OccProb' * (2*(M2 - M1));
   deln_expect(eigen) = OccProb' * l;

   del2_M(eigen) = (OccProb' * (2*(M2 - M1)).^2) - delM_expect(eigen)^2;
   del2_n(eigen) = (OccProb' * (l.^2)) - deln_expect(eigen)^2;

   expect_K(eigen) = c(:,eigen)' * K * c(:,eigen);
```

```
    del2_E(eigen) = c(:,eigen)' * (H.^2) * c(:,eigen) - (c(:,eigen)' * H * c(:,eigen))^2;
    del2_K2(eigen) = c(:,eigen)' * K * K * c(:,eigen);

end


% Want deltaM and deltan not squares necessarily
% ABS added, because above subtractions give a floating point error (~-1e-16)
del2_M = sqrt(abs(del2_M));
del2_n = sqrt(abs(del2_n));
del2_E = sqrt(del2_E);
del2_K = sqrt(del2_K2);
```

Appendix D: PositionMap—Three Dimensional Representation of State Occupation through Matlab Code

```
function [M, X, L] = PositionMap(Basis, u, A);
%
%  Position Map creates a map of the state occupation in two dimensions:
%     with respect to M2-M1 (Position) and l (Photon level).
%     It has three inputs, a basis (Basis), the state occupations (u),
%     and the number of atoms (A)
%
%
%  [M, X, L] = PositionMap(Basis, u, A);
%
%
%  M is a collapsed version of u, each row of u is tied together to make M
%  X is the position vector
%  L is the photon displacement vector
%
%


%  B is the number of states
B = length(Basis);

%  A is number of atoms and x is position vector (-2S:2S)
X = [-A:A];

%  l is a vector of possible n-n0 values.
L = [Basis(B,3):Basis(1,3)];

%  M(L,X) is the matrix with each point of X,L listed with occupation
M = zeros(length(L),length(X));

L_Offset = max(L)+1;  % Since matrices must have positive integer indexes, L must be offset
M_Offset = A+1;  % The minimum l and x is -L and -A, therefore value chosen so that begin with 1

for state = 1:B
   M1 = Basis(state,1);
   M2 = Basis(state,2);
   l = Basis(state,3);

   x = M2 - M1;

   M(l+L_Offset, x+M_Offset) = M(l+L_Offset, x+M_Offset) + (abs(u(state))).^2; %mean((abs(u(state,:)))).^2);
end

figure(4)
surfl(X,L,M);
```

Appendix D: PositionMap—Three Dimensional Representation of State Occupation through Matlab Code

```
shading interp;
colormap(cool);

xlabel('Pseudo-Position (M2 - M1)');
ylabel('Relative Photon Level, (n-n_0)');
zlabel('Probability of Occupation');
```

Appendix E: One-Atom Energy Oscillation Periods v/s Parameters

1-Atom (k = 1)						Data		Advanced II				Advanced I				Simple II				Simple I			
n	g	η	α	$g\sqrt{n}$	l	Slope	Period	Period	Error	MaxSlope	Error	Period	Error	MaxSlope	Error	Period	Error	MaxSlope	Error	Period	Error	MaxSlope	Error
1	1.0000E-02	0.01	10	0.0100	50	1.9915E-06	1.5800E+06	1.6240E+06	0.97290	1.8184E-06	1.09519	1.5079E+06	1.04782	1.9584E-06	1.01689	1.6191E+06	0.97582	1.8239E-06	1.09192	1.8200E+05	8.68132	1.6226E-05	0.12274
1	1.0000E-01	1E-08	10	0.1000	50	1.5073E-10	1.9300E+10	1.9361E+10	0.99684	1.5253E-10	0.98822	1.9038E+10	1.01376	1.5512E-10	0.97173	4.2295E+10	0.45632	6.9821E-11	2.15881	1.8200E+10	1.06044	1.6226E-10	0.92895
1	1.0000E-01	1E-06	10	0.1000	20	1.5073E-08	1.9300E+08	1.9361E+08	0.99684	1.5253E-08	0.98822	1.9038E+08	1.01376	1.5512E-08	0.97173	4.2295E+08	0.45632	6.9821E-09	2.15881	1.8200E+08	1.06044	1.6226E-08	0.92895
1	1.0000E-01	1E-04	10	0.1000	20	1.5073E-06	1.9300E+06	1.9361E+06	0.99684	1.5253E-06	0.98822	1.9038E+06	1.01376	1.5512E-06	0.97173	4.2295E+06	0.45632	6.9821E-07	2.15881	1.8200E+06	1.06044	1.6226E-06	0.92895
1	1.0000E-01	0.001	10	0.1000	20	1.5073E-05	1.9300E+05	1.9361E+05	0.99684	1.5253E-05	0.98822	1.9038E+05	1.01376	1.5512E-05	0.97173	4.2295E+05	0.45632	6.9821E-06	2.15881	1.8200E+05	1.06044	1.6226E-05	0.92895
1	1.0000E-01	0.01	10	0.1000	20	1.5070E-04	1.9300E+04	1.9360E+04	0.99690	1.5254E-04	0.98796	1.9037E+04	1.01381	1.5512E-04	0.97149	4.2295E+04	0.45632	6.9821E-05	2.15838	1.8200E+04	1.06044	1.6226E-04	0.92877
1	1.0000E-01	0.1	10	0.1000	20	1.5000E-03	1.9300E+03	1.9232E+03	1.00353	1.5355E-03	0.97688	1.8947E+03	1.01861	1.5586E-03	0.96242	4.2295E+03	0.45632	6.9821E-04	2.14835	1.8200E+03	1.06044	1.6226E-03	0.92445
1	1.0000E-01	0.3	10	0.1000	30	2.1050E-03	6.0000E+02	6.0665E+02	0.98903	4.8679E-03	0.43243	6.0740E+02	0.98781	4.8618E-03	0.43296	1.4098E+03	0.42558	2.0946E-03	1.00495	6.0667E+02	0.98901	4.8677E-03	0.43244
1	1.0000E-01	0.5	10	0.1000	30	6.6667E-03	3.6000E+02	3.2269E+02	1.11563	9.1516E-03	0.72847	3.3543E+02	1.07324	8.8039E-03	0.75724	8.4590E+02	0.42558	3.4911E-03	1.90964	3.6400E+02	0.98901	8.1129E-03	0.82174
1	1.5811E-01	0.001	10	0.1581	30	2.9243E-05	9.7500E+04	8.9733E+04	1.08655	3.2910E-05	0.88858	1.0503E+05	0.92833	2.8117E-05	1.04004	2.5619E+05	0.38058	1.1527E-05	2.53692	1.1511E+05	0.84704	2.5655E-05	1.13984
10	3.1623E-05	0.001	10	0.0001	25	1.9970E-12	1.5730E+12	1.6200E+12	0.97099	1.8229E-12	1.09551	6.2964E+15	0.00025	4.6902E-16	4257.86	1.5718E+12	1.00078	1.8788E-12	1.06290	1.8200E+09	864.286	1.6226E-09	0.00123
10	6.3246E-05	0.001	10	0.0002	25	7.9538E-12	3.9300E+11	4.0500E+11	0.97037	7.2916E-12	1.09082	3.9443E+14	0.00100	7.4870E-15	1062.34	3.9294E+11	1.00014	7.5153E-12	1.05835	9.1000E+08	431.868	3.2452E-09	0.00245
10	9.4868E-05	0.001	10	0.0003	25	1.7860E-11	1.7400E+11	1.8000E+11	0.96667	1.6406E-11	1.08862	7.8106E+13	0.00223	3.7809E-14	472.375	1.7464E+11	0.99632	1.6909E-11	1.05622	6.0667E+08	286.813	4.8677E-09	0.00367
10	1.2649E-04	0.001	10	0.0004	25	3.1806E-11	9.8400E+10	1.0125E+11	0.97185	2.9166E-11	1.09051	2.4780E+13	0.00397	1.1917E-13	266.886	9.8237E+10	1.00166	3.0061E-11	1.05805	4.5500E+08	216.264	6.4903E-09	0.00490
10	1.5811E-04	0.001	10	0.0005	25	4.9927E-11	6.3000E+10	6.4800E+10	0.97222	4.5572E-11	1.09556	1.0179E+13	0.00619	2.9012E-13	172.093	6.2872E+10	1.00204	4.6970E-11	1.06295	3.6400E+08	173.077	8.1129E-09	0.00615
10	1.8974E-04	0.001	10	0.0006	25	7.1611E-11	4.3700E+10	4.5000E+10	0.97110	6.5624E-11	1.09123	4.9240E+12	0.00887	5.9974E-13	119.404	4.3661E+10	1.00089	6.7637E-11	1.05875	3.0333E+08	144.066	9.7355E-09	0.00736
10	2.2136E-04	0.001	10	0.0007	25	9.7906E-11	3.1000E+10	3.3062E+10	0.93764	8.9321E-11	1.09611	2.6665E+12	0.01163	1.1075E-12	88.4056	3.2078E+10	0.96641	9.2061E-11	1.06349	2.6000E+08	119.231	1.1358E-08	0.00862
10	2.5298E-04	0.001	10	0.0008	25	1.2722E-10	2.4600E+10	2.5313E+10	0.97184	1.1666E-10	1.09048	1.5685E+12	0.01568	1.8828E-12	67.5712	2.4560E+10	1.00165	1.2024E-10	1.05803	2.2750E+08	108.132	1.2981E-08	0.00980
10	2.8460E-04	0.001	10	0.0009	25	1.6117E-10	1.9400E+10	2.0000E+10	0.96998	1.4765E-10	1.09155	9.8279E+11	0.01974	3.0048E-12	53.6374	1.9405E+10	0.99973	1.5218E-10	1.05907	2.0222E+08	95.9341	1.4603E-08	0.01104
10	3.1623E-04	0.001	10	0.0010	25	1.9945E-10	1.5700E+10	1.6200E+10	0.96911	1.8229E-10	1.09416	6.4729E+11	0.02425	4.5622E-12	43.7177	1.5718E+10	0.99884	1.8788E-10	1.06160	1.8200E+08	86.2637	1.6226E-08	0.01229
10	9.4868E-04	0.001	10	0.0030	25	1.79E-09	1.7500E+09	1.8004E+09	0.97200	1.6402E-09	1.09131	8.9625E+09	0.19526	3.2950E-10	5.43253	1.7469E+09	1.00177	1.6905E-09	1.05888	6.0667E+07	28.8462	4.8677E-08	0.03677
10	1.5811E-03	0.001	10	0.0050	25	4.9908E-09	6.2950E+08	6.4841E+08	0.97083	4.5544E-09	1.09583	1.3823E+09	0.45540	2.1364E-09	2.33612	6.2920E+08	1.00047	4.6934E-09	1.06337	3.6400E+07	17.2940	8.1129E-08	0.06152
10	2.5298E-03	0.001	10	0.0080	25	1.2647E-08	2.4650E+08	2.5354E+08	0.97224	1.1648E-08	1.08580	2.9182E+08	0.84469	1.0119E-08	1.24977	2.4608E+08	1.00170	1.2001E-08	1.05387	2.2750E+07	10.8352	1.2981E-07	0.09743
10	3.1623E-03	0.001	10	0.0100	25	1.9931E-08	1.5700E+08	1.6241E+08	0.96668	1.8183E-08	1.09615	1.5080E+08	1.04114	1.9583E-08	1.01775	1.5767E+08	0.99576	1.8730E-08	1.06413	1.8200E+07	8.62637	1.6226E-07	0.12284
10	1.0000E-02	0.01	10	0.0316	20	1.9549E-06	1.6000E+06	1.6598E+06	0.96398	1.7792E-06	1.09875	1.1282E+06	1.41816	2.6175E-06	0.74686	1.6202E+06	0.98756	1.8227E-06	1.07251	5.7553E+05	2.78002	5.1311E-06	0.38099
10	3.1623E-02	1E-06	10	0.1000	20	1.6449E-09	1.8250E+09	1.9361E+09	0.94260	1.5253E-09	1.07844	1.9038E+09	0.95861	1.5512E-09	1.06044	2.0036E+09	0.91085	1.4739E-09	1.11604	1.8200E+09	1.00275	1.6226E-09	1.01376

Appendix E: One-Atom Energy Oscillation Periods v/s Parameters

10	3.1623E-02	1E-04	10	0.1000	20	1.6449E-07	1.8250E+07	1.9361E+07	0.94260	1.5253E-07	1.07844	1.9038E+07	0.95861	1.5512E-07	1.06044	2.0036E+07	0.91085	1.4739E-07	1.11604	1.8200E+07	1.00275	1.6226E-07	1.01376
10	3.1623E-02	0.001	10	0.1000	20	1.6449E-06	1.8250E+06	1.9361E+06	0.94261	1.5253E-06	1.07844	1.9038E+06	0.95861	1.5512E-06	1.06044	2.0036E+06	0.91085	1.4739E-06	1.11604	1.8200E+06	1.00275	1.6226E-06	1.01376
10	3.1623E-02	0.01	10	0.1000	20	1.6451E-05	1.8250E+05	1.9360E+05	0.94267	1.5254E-05	1.07850	1.9037E+05	0.95865	1.5512E-05	1.06051	2.0036E+05	0.91085	1.4739E-05	1.11617	1.8200E+05	1.00275	1.6226E-05	1.01388
10	3.1623E-02	0.1	10	0.1000	20	1.6605E-04	1.8180E+04	1.9232E+04	0.94529	1.5355E-04	1.08141	1.8947E+04	0.95950	1.5586E-04	1.06539	2.0036E+04	0.90735	1.4739E-04	1.12662	1.8200E+04	0.99890	1.6226E-04	1.02337
10	3.1623E-02	0.3	.1	0.1000	20	4.4444E-04	5.6200E+03	6.0665E+03	0.92640	4.8679E-04	0.91302	6.0740E+03	0.92525	4.8618E-04	0.91415	6.6788E+03	0.84147	4.4216E-04	1.00516	6.0667E+03	0.92637	4.8677E-04	0.91304
10	3.1623E-02	0.5	.1	0.1000	20	9.7561E-04	3.2300E+03	3.2269E+03	1.00097	9.1516E-04	1.06606	3.3543E+03	0.96294	8.8039E-04	1.10816	4.0073E+03	0.80604	7.3694E-04	1.32387	3.6400E+03	0.88736	8.1129E-04	1.20254
10	1.5811E-01	0.001	10	0.5000	30	6.8693E-06	2.3700E+05	1.6360E+05	1.44869	1.8051E-05	0.38055	2.7657E+05	0.85692	1.0678E-05	0.64334	2.5635E+05	0.92452	1.1520E-05	0.59630	3.6400E+05	0.65110	8.1129E-06	0.84671
10	2.2136E-01	0.001	10	0.7000	20	7.5000E-06	1.7600E+05	1.0731E+05	1.64005	2.7518E-05	0.27254	1.9238E+05	0.91485	1.5350E-05	0.48859	1.8039E+05	0.97567	1.6371E-05	0.45814	2.6000E+05	0.67692	1.1358E-05	0.66032
10	3.1623E-01	0.001	10	1.0000	30	7.6952E-06	1.2000E+05	7.2629E+04	1.65223	4.0660E-05	0.18926	1.3196E+05	0.90937	2.2379E-05	0.34386	1.2525E+05	0.95808	2.3578E-05	0.32638	1.8200E+05	0.65934	1.6226E-05	0.47426
10	6.3246E-01	0.001	10	2.0000	25	8.5000E-06	5.7000E+04	4.0525E+04	1.40653	7.2871E-05	0.11665	6.4404E+04	0.88504	4.5853E-05	0.18538	6.2254E+04	0.91560	4.7436E-05	0.17919	9.1000E+04	0.62637	3.2452E-05	0.26193
100	1.0000E-02	1E-08	10	0.1000	25	1.6596E-12	1.8200E+12	1.9361E+12	0.94002	1.5253E-12	1.08808	1.9038E+12	0.95598	1.5512E-12	1.06991	1.7120E+12	1.06306	1.7249E-12	0.96214	1.8200E+12	1.00000	1.6226E-12	1.02281
100	1.0000E-02	1E-06	10	0.1000	20	1.6596E-10	1.8200E+10	1.9361E+10	0.94002	1.5253E-10	1.08808	1.9038E+10	0.95598	1.5512E-10	1.06991	1.7120E+10	1.06306	1.7249E-10	0.96214	1.8200E+10	1.00000	1.6226E-10	1.02281
100	1.0000E-02	1E-04	10	0.1000	20	1.6596E-08	1.8200E+08	1.9361E+08	0.94002	1.5253E-08	1.08808	1.9038E+08	0.95598	1.5512E-08	1.06991	1.7120E+08	1.06306	1.7249E-08	0.96214	1.8200E+08	1.00000	1.6226E-08	1.02281
100	1.0000E-02	0.001	10	0.1000	20	1.6596E-07	1.8200E+07	1.9361E+07	0.94002	1.5253E-07	1.08807	1.9038E+07	0.95598	1.5512E-07	1.06991	1.7120E+07	1.06306	1.7249E-07	0.96214	1.8200E+07	1.00000	1.6226E-07	1.02281
100	1.0000E-02	0.01	10	0.1000	20	1.6597E-06	1.8200E+06	1.9360E+06	0.94009	1.5254E-06	1.08807	1.9037E+06	0.95603	1.5512E-06	1.06993	1.7120E+06	1.06306	1.7249E-06	0.96220	1.8200E+06	1.00000	1.6226E-06	1.02288
100	1.0000E-02	0.05	10	0.1000	20	8.3108E-06	3.6300E+05	3.8658E+05	0.93900	7.6390E-06	1.08794	3.8031E+05	0.95449	7.7650E-06	1.07029	3.4241E+05	1.06014	8.6245E-06	0.96362	3.6400E+05	0.99725	8.1129E-06	1.02439
100	1.0000E-02	0.08	10	0.1000	20	1.3329E-05	2.2600E+05	2.4098E+05	0.93783	1.2254E-05	1.08769	2.3725E+05	0.95258	1.2447E-05	1.07085	2.1400E+05	1.05606	1.3799E-05	0.96592	2.2750E+05	0.99341	1.2981E-05	1.02684
100	1.0000E-02	0.1	10	0.1000	20	1.6697E-05	1.8100E+05	1.9232E+05	0.94113	1.5355E-05	1.08740	1.8947E+05	0.95528	1.5586E-05	1.07130	1.7120E+05	1.05722	1.7249E-05	0.96799	1.8200E+05	0.99451	1.6226E-05	1.02904
100	1.0000E-02	0.2	10	0.1000	20	3.4161E-05	8.8000E+04	9.4225E+04	0.93394	3.1341E-05	1.08998	9.3377E+04	0.94242	3.1625E-05	1.08017	8.5602E+04	1.02802	3.4498E-05	0.99023	9.1000E+04	0.96703	3.2452E-05	1.05267
100	1.0000E-02	0.3	10	0.1000	20	5.3709E-05	5.5400E+04	6.0665E+04	0.91321	4.8679E-05	1.10334	6.0740E+04	0.91208	4.8618E-05	1.10471	5.7068E+04	0.97078	5.1747E-05	1.03791	6.0667E+04	0.91319	4.8677E-05	1.10337
100	1.0000E-02	0.4	10	0.1000	20	6.8190E-05	4.2900E+04	4.3240E+04	0.99213	6.8295E-05	0.99846	4.3969E+04	0.97569	6.7163E-05	1.01528	4.2801E+04	1.00232	6.8996E-05	0.98831	4.5500E+04	0.94286	6.4903E-05	1.05064
100	1.0000E-02	0.5	10	0.1000	20	9.4014E-05	3.1100E+04	3.2269E+04	0.96378	9.1516E-05	1.02730	3.3543E+04	0.92716	8.8039E-05	1.06787	3.4241E+04	0.90828	8.6245E-05	1.09008	3.6400E+04	0.85440	8.1129E-05	1.15882
100	1.0000E-02	0.6	10	0.1000	20	1.1142E-04	2.4000E+04	2.4524E+04	0.97862	1.2042E-04	0.92530	2.6291E+04	0.91287	1.1233E-04	0.99194	2.8534E+04	0.84111	1.0349E-04	1.07658	3.0333E+04	0.79121	9.7355E-05	1.14447
100	1.0000E-02	0.7	10	0.1000	20	1.2395E-04	1.9700E+04	1.8624E+04	1.05779	1.5857E-04	0.78169	2.0851E+04	0.94479	1.4163E-04	0.87518	2.4458E+04	0.80548	1.2074E-04	1.02656	2.6000E+04	0.75769	1.1358E-04	1.09129
100	1.0000E-02	0.8	10	0.1000	20	1.1667E-04	1.7200E+04	1.3876E+04	1.23959	2.1283E-04	0.54818	1.6545E+04	1.03959	1.7849E-04	0.65363	2.1400E+04	0.80372	1.3799E-04	0.84546	2.2750E+04	0.75604	1.2981E-04	0.89877
100	1.5811E-01	0.001	10	1.5811	30	7.5000E-07	8.1000E+05	4.8253E+05	1.67864	6.1200E-06	0.12255	8.1993E+05	0.98789	3.6016E-06	0.20824	2.7089E+05	2.99018	1.0902E-05	0.06880	1.1511E+06	0.70369	2.5655E-06	0.29234
1000	3.1623E-03	1E-06	10	0.1000	30	1.6570E-11	1.8200E+11	1.9361E+11	0.94002	1.5253E-11	1.08637	1.9038E+11	0.95598	1.5512E-11	1.06824	3.5581E+11	0.51151	8.2997E-12	1.99646	1.8200E+11	1.00000	1.6226E-11	1.02121
1000	3.1623E-03	1E-04	10	0.1000	30	1.6571E-09	1.8200E+09	1.9361E+09	0.94002	1.5253E-09	1.08644	1.9038E+09	0.95598	1.5512E-09	1.06830	3.5581E+09	0.51151	8.2997E-10	1.99658	1.8200E+09	1.00000	1.6226E-09	1.02127
1000	3.1623E-03	0.001	10	0.1000	30	1.6571E-08	1.8200E+08	1.9361E+08	0.94002	1.5253E-08	1.08644	1.9038E+08	0.95598	1.5512E-08	1.06830	3.5581E+08	0.51151	8.2997E-09	1.99658	1.8200E+08	1.00000	1.6226E-08	1.02127

Appendix E: One-Atom Energy Oscillation Periods v/s Parameters

1000	3.1623E-03	0.01	10	0.1000	30	1.6573E-07	1.8200E+07	1.9360E+07	0.94009	1.5254E-07	1.08649	1.9037E+07	0.95603	1.5512E-07	1.06838	3.5581E+07	0.51151	8.2997E-08	1.99682	1.8200E+07	1.00000	1.6226E-07	1.02140
1000	3.1623E-03	0.1	10	0.1000	30	1.6701E-06	1.8050E+06	1.9232E+06	0.93853	1.5355E-06	1.08766	1.8947E+06	0.95264	1.5586E-06	1.07155	3.5581E+06	0.50730	8.2997E-07	2.01225	1.8200E+06	0.99176	1.6226E-06	1.02929
1000	3.1623E-03	0.5	10	0.1000	30	9.4126E-06	3.1000E+05	3.2269E+05	0.96068	9.1516E-06	1.02852	3.3543E+05	0.92418	8.8039E-06	1.06915	7.1162E+05	0.43563	4.1498E-06	2.26818	3.6400E+05	0.85165	8.1129E-06	1.16020
1000	1.0000E-02	0.01	10	0.3162	30	6.5264E-07	3.6700E+06	3.0941E+06	1.18614	9.5444E-07	0.68380	4.6065E+06	0.79669	6.4107E-07	1.01805	3.6562E+06	1.00378	8.0770E-07	0.80802	5.7553E+06	0.63767	5.1311E-07	1.27194
1000	1.5811E-01	0.001	10	5.0000	60	4.6667E-08	2.8500E+06	2.3366E+06	1.21971	1.2638E-06	0.03692	2.5384E+06	1.12275	1.1634E-06	0.04011	5.7850E+05	4.92653	5.1047E-06	0.00914	3.6400E+06	0.78297	8.1129E-07	0.05752
10000	1.0000E-03	1E-06	10	0.1000	25	1.6608E-12	1.8200E+12	1.9361E+12	0.94002	1.5253E-12	1.08886	1.9038E+12	0.95598	1.5512E-12	1.07069	1.1112E+13	0.16379	2.6576E-13	6.24919	1.8200E+12	1.00000	1.6226E-12	1.02355
10000	1.0000E-03	1E-04	10	0.1000	25	1.6608E-10	1.8200E+10	1.9361E+10	0.94002	1.5253E-10	1.08886	1.9038E+10	0.95598	1.5512E-10	1.07069	1.1112E+11	0.16379	2.6576E-11	6.24919	1.8200E+10	1.00000	1.6226E-10	1.02355
10000	1.0000E-03	0.001	10	0.1000	25	1.6608E-09	1.8200E+09	1.9361E+09	0.94002	1.5253E-09	1.08886	1.9038E+09	0.95598	1.5512E-09	1.07069	1.1112E+10	0.16379	2.6576E-10	6.24919	1.8200E+09	1.00000	1.6226E-09	1.02355
10000	1.0000E-03	0.01	10	0.1000	25	1.6609E-08	1.8200E+08	1.9360E+08	0.94009	1.5254E-08	1.08885	1.9037E+08	0.95603	1.5512E-08	1.07070	1.1112E+09	0.16379	2.6576E-09	6.24956	1.8200E+08	1.00000	1.6226E-08	1.02362
10000	1.0000E-03	0.1	10	0.1000	25	1.6730E-07	1.8000E+07	1.9232E+07	0.93593	1.5355E-07	1.08955	1.8947E+07	0.95000	1.5586E-07	1.07342	1.1112E+08	0.16199	2.6576E-08	6.29509	1.8200E+07	0.98901	1.6226E-07	1.03107
10000	1.0000E-03	0.5	10	0.1000	25	9.3190E-07	3.1000E+06	3.2269E+06	0.96068	9.1516E-07	1.01829	3.3543E+06	0.92418	8.8039E-07	1.05851	2.2224E+07	0.13949	1.3288E-07	7.01303	3.6400E+06	0.85165	8.1129E-07	1.14866
10000	1.0000E-02	0.01	10	1.0000		7.7500E-08	1.2400E+07	7.2624E+06	1.70742	4.0663E-07	0.19059	1.3195E+07	0.93972	2.2380E-07	0.34629	1.1450E+07	1.08295	2.5791E-07	0.30049	1.8200E+07	0.68132	1.6226E-07	0.47763
10000	1.5811E-01	0.001	10	15.811		4.0000E-09	1.6200E+07	1.2909E+07	1.25491	2.2876E-07	0.01749	7.9728E+06	2.03191	3.7040E-07	0.01080	1.8117E+06	8.94182	1.6300E-06	0.00245	1.1511E+07	1.40739	2.5655E-07	0.01559
30000	1.0000E-02	0.01	10	1.7321		2.1500E-08	2.1000E+07	1.3495E+07	1.55619	2.1884E-07	0.09825	2.2394E+07	0.93777	1.3187E-07	0.16304	1.9831E+07	1.05897	1.4892E-07	0.14438	3.1523E+07	0.66617	9.3680E-08	0.22951
50000	1.0000E-02	0.01	10	2.2361	80	1.2000E-08	2.8000E+07	1.8772E+07	1.49155	1.5731E-07	0.07628	2.8727E+07	0.97470	1.0280E-07	0.11673	2.5601E+07	1.09371	1.1535E-07	0.10403	4.0696E+07	0.68802	7.2564E-08	0.16537
80000	1.0000E-02	0.01	10	2.8284	60	1.3362E-08	3.5710E+07	2.5853E+07	1.38126	1.1423E-07	0.11698	3.6170E+07	0.98728	8.1645E-08	0.16366	3.2383E+07	1.10274	9.1193E-08	0.14652	5.1477E+07	0.69370	5.7367E-08	0.23292
100000	1.0000E-02	0.01	10	3.1623	100	7.8570E-09	3.9000E+07	3.0220E+07	1.29055	9.7721E-08	0.08040	4.0365E+07	0.96618	7.3160E-08	0.10740	3.6205E+07	1.07720	8.1566E-08	0.09633	5.7553E+07	0.67763	5.1311E-08	0.15313
200000	1.0000E-02	0.01	10	4.4721	100	3.2660E-09	5.5000E+07	4.9649E+07	1.10778	5.9480E-08	0.05491	5.6824E+07	0.96789	5.1969E-08	0.08285	5.1202E+07	1.07418	5.7676E-08	0.05663	8.1393E+07	0.67573	3.6282E-08	0.09002
300000	1.0000E-02	0.01	10	5.4772	100	1.4290E-09	6.7000E+07	6.6755E+07	1.00367	4.4238E-08	0.03230	6.9454E+07	0.96467	4.2519E-08	0.03361	6.2709E+07	1.06843	4.7092E-08	0.03034	9.9686E+07	0.67211	2.9624E-08	0.04824
500000	1.0000E-02	0.01	10	7.0711	100	8.3333E-10	9.3000E+07	9.7283E+07	0.95598	3.0356E-08	0.02745	8.9482E+07	1.03932	3.3002E-08	0.02525	8.0957E+07	1.14876	3.6477E-08	0.02285	1.2869E+08	0.72265	2.2947E-08	0.03632
600000	1.0000E-02	0.01	10	7.7460	100	5.0000E-10	1.0700E+08	1.1135E+08	0.96090	2.6520E-08	0.01885	9.7963E+07	1.09225	3.0145E-08	0.01659	8.8684E+07	1.20653	3.3299E-08	0.01502	1.4098E+08	0.75899	2.0947E-08	0.02387
800000	1.0000E-02	0.01	10	8.9443	100	4.1667E-10	1.4500E+08	1.3788E+08	1.05161	2.1417E-08	0.01945	1.1302E+08	1.28296	2.6129E-08	0.01595	1.0240E+08	1.41597	2.8838E-08	0.01445	1.6279E+08	0.89074	1.8141E-08	0.02297
900000	1.0000E-02	0.01	10	9.4868	100	3.3333E-10	1.8000E+08	1.5051E+08	1.19590	1.9620E-08	0.01699	1.1984E+08	1.50203	2.4642E-08	0.01353	1.0862E+08	1.65723	2.7189E-08	0.01226	1.7266E+08	1.04251	1.7104E-08	0.01949
1000000	1.0000E-04	1E-06	10	0.1000	20	1.6130E-14	1.8800E+14	1.9361E+14	0.97101	1.5253E-14	1.05752	1.9038E+14	0.98750	1.5512E-14	1.03987	1.1107E+16	0.01693	2.6587E-16	60.6684	1.8200E+14	1.03297	1.6226E-14	0.99410
1000000	1.0000E-04	1E-04	10	0.1000	20	1.6522E-12	1.8380E+12	1.9361E+12	0.94932	1.5253E-12	1.08322	1.9038E+12	0.96543	1.5512E-12	1.06514	1.1107E+14	0.01655	2.6587E-14	62.1428	1.8200E+12	1.00989	1.6226E-12	1.01825
1000000	1.0000E-04	0.001	10	0.1000	20	1.6520E-11	1.8150E+11	1.9361E+11	0.93744	1.5253E-11	1.08309	1.9038E+11	0.95335	1.5512E-11	1.06501	1.1107E+13	0.01634	2.6587E-13	62.1353	1.8200E+11	0.99725	1.6226E-11	1.01813
1000000	1.0000E-04	0.01	10	0.1000	20	1.7089E-10	1.8050E+10	1.9360E+10	0.93235	1.5254E-10	1.12030	1.9037E+10	0.94815	1.5512E-10	1.10164	1.1107E+12	0.01625	2.6587E-12	64.2755	1.8200E+10	0.99176	1.6226E-10	1.05320
1000000	1.0000E-04	0.1	10	0.1000	20	1.6392E-09	1.8700E+09	1.9200E+09	0.97396	1.5381E-09	1.06574	1.8947E+09	0.98694	1.5586E-09	1.05173	1.1107E+11	0.01684	2.6587E-11	61.6539	1.8200E+09	1.02747	1.6226E-09	1.01024
1000000	1.0000E-04	0.5	10	0.1000	20	9.3775E-09	3.0300E+08	3.2269E+08	0.93899	9.1516E-09	1.02469	3.3543E+08	0.90331	8.8039E-09	1.06516	2.2214E+10	0.01364	1.3294E-10	70.5416	3.6400E+08	0.83242	8.1129E-09	1.15587

Appendix E: One-Atom Energy Oscillation Periods v/s Parameters

1000000	1.0000E-02	0.01	10	10		1.6667E-10	2.0000E+08	1.6280E+08	1.22849	1.8139E-08	0.00919	1.2629E+08	1.58371	2.3384E-08	0.00713	1.1449E+08	1.74687	2.5793E-08	0.00646	1.8200E+08	1.09890	1.6226E-08	0.01027
1000000	1.5811E-01	0.001	10	158.11			1.6000E+07	4.0742E+08	0.03927	7.2484E-09	0.00000	7.9502E+07	0.20125	3.7145E-08	0.00000	1.8115E+07	0.88323	1.6302E-07	0.00000	1.1511E+08	0.13900	2.5655E-08	0.00000
							Sum of % Divergence	10.6243		24.5374		18.4837		6621.68		38.0091		443.608		2595.87		34.6556	
							Number not within 10%	19		28		23		41		42		54		44		48	

Appendix F: Three-Atom Energy Oscillation Periods v/s Parameters

3-Atom (k = 1)						Data		Advanced II				1-Atom Data		% of 1-Atom	
n	g	η	α	$g\sqrt{n}$	l	Slope	Period	Period	Error	MaxSlope	Error	Slope	Period	Slope	Period
1	1.0000E-02	0.01	10	0.0100	20	8.1703E-06	1.5750E+06	1.6240E+06	0.96982	7.2736E-06	1.12328	1.9915E-06	1.5800E+06	410.26%	99.68%
1	1.0000E-01	1E-08	10	0.1000	30	6.0300E-10	1.9380E+10	1.9361E+10	1.00097	6.1010E-10	0.98835	1.5073E-10	1.9300E+10	400.05%	100.41%
1	1.0000E-01	1E-06	10	0.1000	30	6.0275E-08	1.9380E+08	1.9361E+08	1.00097	6.1010E-08	0.98794	1.5073E-08	1.9300E+08	399.89%	100.41%
1	1.0000E-01	1E-04	10	0.1000	30	6.0300E-06	1.9380E+06	1.9361E+06	1.00097	6.1010E-06	0.98835	1.5073E-06	1.9300E+06	400.05%	100.41%
1	1.0000E-01	0.001	10	0.1000	30	6.0276E-05	1.9380E+05	1.9361E+05	1.00097	6.1011E-05	0.98796	1.5073E-05	1.9300E+05	399.89%	100.41%
1	1.0000E-01	0.01	10	0.1000	30	6.0316E-04	1.9380E+04	1.9360E+04	1.00104	6.1015E-04	0.98855	1.5070E-04	1.9300E+04	400.24%	100.41%
1	1.0000E-01	0.1	10	0.1000	30	7.1121E-03	1.6250E+03	1.9232E+03	0.84494	6.1420E-03	1.15795	1.5000E-03	1.9300E+03	474.14%	84.20%
1	1.0000E-01	0.3	10	0.1000	30	2.1065E-02	1.6800E+02	6.0665E+02	0.27693	1.9471E-02	1.08184	2.1050E-03	6.0000E+02	1000.71%	28.00%
1	1.0000E-01	0.5	10	0.1000	30	3.2697E-02	2.2000E+02	3.2269E+02	0.68177	3.6606E-02	0.89321	6.6667E-03	3.6000E+02	490.46%	61.11%
10	3.1623E-02	1E-08	10	0.1000	30	6.4430E-11	1.8300E+11	1.9361E+11	0.94519	6.1010E-11	1.05605				
10	3.1623E-02	1E-06	10	0.1000	30	6.4400E-09	1.8300E+09	1.9361E+09	0.94519	6.1010E-09	1.05556	1.6449E-09	1.8250E+09	391.51%	100.27%
10	3.1623E-02	1E-04	10	0.1000	30	6.4430E-07	1.8300E+07	1.9361E+07	0.94519	6.1010E-07	1.05605	1.6449E-07	1.8250E+07	391.70%	100.27%
10	3.1623E-02	0.001	10	0.1000	30	6.4430E-06	1.8250E+06	1.9361E+06	0.94261	6.1011E-06	1.05605	1.6449E-06	1.8250E+06	391.70%	100.00%
10	3.1623E-02	0.01	10	0.1000	30	6.4440E-05	1.8250E+05	1.9360E+05	0.94267	6.1015E-05	1.05614	1.6451E-05	1.8250E+05	391.71%	100.00%
10	3.1623E-02	0.1	10	0.1000	30	6.4480E-04	1.8150E+04	1.9232E+04	0.94373	6.1420E-04	1.04982	1.6605E-04	1.8180E+04	388.32%	99.83%
10	3.1623E-02	0.3	0.1	0.1000	30	2.8436E-03	5.5250E+03	6.0665E+03	0.91074	1.9471E-03	1.46040	4.4444E-04	5.6200E+03	639.81%	98.31%
10	3.1623E-02	0.5	0.1	0.1000	30	4.1742E-03	3.2250E+03	3.2269E+03	0.99942	3.6606E-03	1.14030	9.7561E-04	3.2300E+03	427.86%	99.85%
100	1.0000E-02	1E-08	10	0.1000	50	6.4948E-12	1.8200E+12	1.9361E+12	0.94002	6.1010E-12	1.06454	1.6596E-12	1.8200E+12	391.35%	100.00%
100	1.0000E-02	1E-06	10	0.1000	50	6.4949E-10	1.8200E+10	1.9361E+10	0.94002	6.1010E-10	1.06455	1.6596E-10	1.8200E+10	391.35%	100.00%
100	1.0000E-02	1E-04	10	0.1000	50	6.4949E-08	1.8150E+08	1.9361E+08	0.93744	6.1010E-08	1.06455	1.6596E-08	1.8200E+08	391.35%	99.73%
100	1.0000E-02	0.001	10	0.1000	50	6.4948E-07	1.8150E+07	1.9361E+07	0.93744	6.1011E-07	1.06454	1.6596E-07	1.8200E+07	391.35%	99.73%
100	1.0000E-02	0.01	10	0.1000	50	6.4912E-06	1.8150E+06	1.9360E+06	0.93750	6.1015E-06	1.06388	1.6597E-06	1.8200E+06	391.11%	99.73%
100	1.0000E-02	0.1	10	0.1000	50	6.5266E-05	1.8050E+05	1.9232E+05	0.93853	6.1420E-05	1.06262	1.6697E-05	1.8100E+05	390.88%	99.72%
100	1.0000E-02	0.3	10	0.1000	50	2.0755E-04	5.5400E+04	6.0665E+04	0.91321	1.9471E-04	1.06592	5.3709E-05	5.5400E+04	386.43%	100.00%
100	1.0000E-02	0.5	10	0.1000	50	3.6424E-04	3.1200E+04	3.2269E+04	0.96688	3.6606E-04	0.99502	9.4014E-05	3.1100E+04	387.43%	100.32%
1000	3.1623E-03	1E-08	10	0.1000	50	6.4983E-13	1.8150E+13	1.9361E+13	0.93744	6.1010E-13	1.06511				

Appendix F: Three-Atom Energy Oscillation Periods v/s Parameters

1000	3.1623E-03	1E-06	10	0.1000	50	6.4963E-11	1.8150E+11	1.9361E+11	0.93744	6.1010E-11	1.06478	1.6570E-11	1.8200E+11	392.05%	99.73%
1000	3.1623E-03	1E-04	10	0.1000	50	6.4963E-09	1.8100E+09	1.9361E+09	0.93486	6.1010E-09	1.06478	1.6571E-09	1.8200E+09	392.03%	99.45%
1000	3.1623E-03	0.001	10	0.1000	50	6.4968E-08	1.8100E+08	1.9361E+08	0.93486	6.1011E-08	1.06487	1.6571E-08	1.8200E+08	392.06%	99.45%
1000	3.1623E-03	0.01	10	0.1000	50	6.4899E-07	1.8100E+07	1.9360E+07	0.93492	6.1015E-07	1.06366	1.6573E-07	1.8200E+07	391.59%	99.45%
1000	3.1623E-03	0.1	10	0.1000	50	6.5287E-06	1.8000E+06	1.9232E+06	0.93593	6.1420E-06	1.06296	1.6701E-06	1.8050E+06	390.92%	99.72%
1000	3.1623E-03	0.3	10	0.1000	50	2.0440E-05	5.5300E+05	6.0665E+05	0.91156	1.9471E-05	1.04974				
1000	3.1623E-03	0.5	10	0.1000	50	3.4745E-05	3.1100E+05	3.2269E+05	0.96378	3.6606E-05	0.94915	9.4126E-06	3.1000E+05	369.13%	100.32%
10000	1.0000E-03	1E-08	10	0.1000	50	6.5297E-14	1.8150E+14	1.9361E+14	0.93744	6.1010E-14	1.07026				
10000	1.0000E-03	1E-06	10	0.1000	50	6.5068E-12	1.8150E+12	1.9361E+12	0.93744	6.1010E-12	1.06651	1.6608E-12	1.8200E+12	391.79%	99.73%
10000	1.0000E-03	1E-04	10	0.1000	50	6.5065E-10	1.8150E+10	1.9361E+10	0.93744	6.1010E-10	1.06646	1.6608E-10	1.8200E+10	391.77%	99.73%
10000	1.0000E-03	0.001	10	0.1000	50	6.5077E-09	1.8150E+09	1.9361E+09	0.93744	6.1011E-09	1.06665	1.6608E-09	1.8200E+09	391.84%	99.73%
10000	1.0000E-03	0.01	10	0.1000	50	6.4831E-08	1.8150E+08	1.9360E+08	0.93750	6.1015E-08	1.06255	1.6609E-08	1.8200E+08	390.34%	99.73%
10000	1.0000E-03	0.1	10	0.1000	50	6.5363E-07	1.8000E+07	1.9232E+07	0.93593	6.1420E-07	1.06420	1.6730E-07	1.8000E+07	390.69%	100.00%
10000	1.0000E-03	0.3	10	0.1000	50	2.0497E-06	5.5300E+06	6.0665E+06	0.91156	1.9471E-06	1.05267				
10000	1.0000E-03	0.5	10	0.1000	50	3.3853E-06	3.1000E+06	3.2269E+06	0.96068	3.6606E-06	0.92479	9.3190E-07	3.1000E+06	363.27%	100.00%
1000000	1.0000E-04	1E-06	10	0.1000	50	6.4957E-14	1.8000E+14	1.9361E+14	0.92969	6.1010E-14	1.06469	1.6130E-14	1.8800E+14	402.71%	95.74%
1000000	1.0000E-04	1E-04	10	0.1000	50	6.4601E-12	1.8150E+12	1.9361E+12	0.93744	6.1010E-12	1.05885	1.6522E-12	1.8380E+12	391.00%	98.75%
1000000	1.0000E-04	0.001	10	0.1000	50	6.5808E-11	1.8100E+11	1.9361E+11	0.93486	6.1011E-11	1.07863	1.6520E-11	1.8150E+11	398.35%	99.72%
							Sum of % Divergence	3.3575		3.128				129.591	0.016
							Number not within 10%	3		5				39	3

REFERENCES

Dicke, R. H., (1954). Coherence in Spontaneous Radiation Processes. Physical Review, 93, 99-110.

Griffiths, David J. (1995). Introduction to Quantum Mechanics. Englewood Cliffs, NJ: Prentice Hall.

Hagelstein, Peter L. (1998). Submitted to Physical Review A.

Hagelstein, Peter L. (1999). Possibility of Off-Resonant Superradiant Effects. In Institute of Physics Conference Series No 159 [Proceedings of the conference X-ray Lasers] (pp. 255-261). Kyoto, Japan: IOP Publishing Ltd.

Hagelstein, Peter L. (2000). Photoelectric Effect Induced by Microwaves. (Unpublished).

INDEX